M. G. Lee, L. P. Zhang, Z. C. Li, A. L. Kazakov, Dual null field method for Dirichlet problems of Laplace's equation in circular domains with circular holes, *Сиб. электрон. матем. изв.*, 2021, том 18, выпуск 1, 393–422

DOI: 10.33048/semi.2021.18.028

S©MR ISSN 1813-3304

СИБИРСКИЕ ЭЛЕКТРОННЫЕ
МАТЕМАТИЧЕСКИЕ ИЗВЕСТИЯ

Siberian Electronic Mathematical Reports

http://semr.math.nsc.ru

Том 18, №1, стр. 393–422 (2021) УДК 519.63

DOI 10.33048/semi.2021.18.028 MSC 65M38

DUAL NULL FIELD METHOD FOR DIRICHLET PROBLEMS OF LAPLACE'S EQUATION IN CIRCULAR DOMAINS WITH CIRCULAR HOLES

M.G. LEE, L.P. ZHANG, Z.C. LI, A.L. KAZAKOV

Abstract. The dual techniques have been widely used in many engineering papers, to deal with singularity and ill-conditioning of the boundary element method (BEM). In this paper, we consider Laplace's equation with circular domains with one circular hole. The explicit algebraic equations of the first and second kinds of the null field method (NFM) are provided for applications. Traditionally, the first and the second kinds of the NFM are used for the Dirichlet and the Neumann problems, respectively. To bypass the degenerate scales of Dirichlet problems, however, the second and the first kinds of the NFM are used for the exterior and the interior boundaries, simultaneously, called the dual NFM (DNFM) in this paper. The excellent stability and the optimal convergence rates are explored in this paper. By using the simple Gaussian elimination or the iteration methods, numerical solutions can be easily obtained. Recently, the study on degenerate scales is active, many removal techniques are proposed, where the advanced solution methods may be needed, such as the truncated singular value decomposition (TSVD) and the overdetermined systems. In contrast, the solution methods of the DNFM in this paper are much simpler, with a little risk of the algorithm singularity from degenerate scales.

Keywords: Laplace's equations, dual techniques, null field method, boundary element method, dual null field method.

Lee, M.G., Zhang, L.P., Li, Z.C., Kazakov, A.L., Dual null field method for Dirichlet problems of Laplace's equation in circular domains with circular holes.

The reported study was funded by the Ministry of Science and Technology (MOST), Grant 109-2923-E-216-001- MY3 and RFBR, research project 20-51-S52003.

Received August, 20, 2020, published April, 16, 2021.

1. Introduction

For Dirichlet problems by the boundary element methods (BEM) and the boundary integral equation methods (BIEM), there may exist the algorithm singularity for some geometric domains, to cause a failure in yielding the unique solutions, called the degenerate scale problems (or simply the degenerate scales). To overcome the degenerate scales, the dual techniques were proposed and reported in many engineering papers. A review paper was given in Chen and Hong [4] in 1999, accompanied by 249 references. Also, the dual techniques of BEM were applied to crack singularity in Portela, Aliabadi and Rooke [20]. The algebraic equations can be easily found, and the unique numerical results may be solved by the Gaussian elimination, or iteration methods. In fact, the dual techniques are the early removal techniques to bypass the degenerate scales. The simple solution methods of dual techniques are advantageous over other advanced removal techniques, such as [3, 9, 11, 10]. So far, it seems to exist no strict theoretical analysis for the dual techniques. In this paper, the null field method (NFM) for Laplace's equation is discussed, and the circular domains with one circular hole are confined. The goal is to provide some theoretical analysis for dual techniques of NFM (DNFM), thus to fill some gap between analysis and computation. The algorithm singularity, unique solutions, error bounds, convergence rates, condition numbers, and stability are explored in this paper, while analysis of algorithm singularity of the dual BEM is reported in Chen et al. [5] by using the singular value decomposition (SVD).

In [3, 9, 11, 10], to deal with the degenerate scales for Dirichlet problems, the advanced techniques of solution methods may be solicited, such as the truncated singular value decomposition (TSVD) and the overdetermined systems. There may raise questions: Can the degenerate scales be removed by the NFM itself? Can the simple Gaussian elimination be used, to reach the optimal stability? Based on the Green representation formula (2.9) and its derivatives (2.14) shown later, the first and the second kinds of NFM are derived, respectively, and the explicit computational formulas of the NFM can be derived for circular and elliptic domains (see [10, 14, 21]). In classic algorithms, the first kind NFM is used for Dirichlet problems; the second kind NFM for Neumann problems. The algorithms using both (2.9) and (2.14) together are called the "*dual*" boundary element method (BEM) in [4, 5, 20], and the "*dual*" techniques of NFM (simply denoted as the DNFM) in this paper. For the circular domains with circular holes, the second kind of the NFM (simply as the second kind NFM) are developed in [10] for Neumann problems, with the explicit algebraic equations. The first kind NFM in [14] may also be applied to Neumann problems, and the numerical performance is as good as that of the second kind NFM, see [10]. Hence, the second kind NFM can also be applied for Dirichlet problems. After a study in Section 2, when the second and the first kind NFMs are applied for the exterior and the interior boundaries, respectively, the algorithms of the DNFM have a little risk of the algorithm singularity from degenerate scales. Such algorithms are called the dual techniques (such as the DNFM) in this paper. Not only are the numerical solutions solved easily by the simple Gaussian elimination (or iteration methods), but also the optimal stability can be reached. Note that the algorithms of the DNFM are analogous to those for the mixed problems in [21]. The optimal convergence rates can be achieved by the DNFM. The DNFM can also be applied to eigenvalue problems for circular domains with circular holes [2].

The study on degenerate scale problems is still active, many techniques are proposed to remove the degenerate scales, where the advanced solution methods may be needed, such as the truncated singular value decomposition (TSVD) and the overdetermined systems. Nevertheless, the solution methods of the DNFM in this paper are much simpler, with a little risk of the algorithm singularity from degenerate scales. Interestingly, from the outcome of this paper, the degenerate scales can be removed by the NFM itself via dual techniques.

This paper is organized as follows. In the next section, the first and the second kinds of the NFM are introduced according to [14, 10] for circular domains with one circular hole, and the dual techniques of NFM (denoted as the DNFM) are proposed. In Section 3, the degenerate scales of the DNFM are studied, and in Section 4, the analysis of stability and error is explored. In Section 5, numerical experiments of the DNFM are reported, and in the last section, a few concluding remarks are made.

2. Null Field Methods and Dual Techniques

2.1. **The First Kind NFM.** Consider Laplace's equation in circular domains with one circular hole. The discussions for circular domains with multiple circular holes are similar. Denote the disks S_R and S_{R_1} with radius R and R_1, respectively. Let $S_{R_1} \subset S_R$, and the eccentric circular domains S_R and S_{R_1} have different origins. Define the annular solution domain $S = S_R \setminus S_{R_1}$ with the exterior and the interior boundaries ∂S_R and ∂S_{R_1}. Denote two systems of polar coordinates by (ρ, θ) and $(\bar{\rho}, \bar{\theta})$ with origins $(0, 0)$ and (x_1, y_1) of S_R and S_{R_1}, respectively. There exist the following conversion relations,

$$\rho = \sqrt{(\bar{\rho}\cos\bar{\theta} + x_1)^2 + (\bar{\rho}\sin\bar{\theta} + y_1)^2}, \quad \cos\theta = \frac{\bar{\rho}\sin\bar{\theta} + y_1}{\rho}, \tag{2.1}$$

$$\bar{\rho} = \sqrt{(\rho\cos\theta - x_1)^2 + (\rho\sin\theta - y_1)^2}, \quad \cos\bar{\theta} = \frac{\rho\sin\theta - y_1}{\bar{\rho}}. \tag{2.2}$$

On the exterior boundary ∂S_R, suppose that there exist the approximations of Fourier expansions,

$$u \approx a_0 + \sum_{k=1}^{M} \{a_k \cos k\theta + b_k \sin k\theta\} \quad \text{on} \quad \partial S_R, \tag{2.3}$$

$$\frac{\partial u}{\partial \nu} \approx \frac{\partial u}{\partial r} = p_0 + \sum_{k=1}^{M} \{p_k \cos k\theta + q_k \sin k\theta\} \quad \text{on} \quad \partial S_R, \tag{2.4}$$

where a_k, b_k, p_k and q_k are coefficients. On the interior boundary ∂S_{R_1}, similarly suppose

$$\bar{u} \approx \bar{a}_0 + \sum_{k=1}^{N} \{\bar{a}_k \cos k\bar{\theta} + \bar{b}_k \sin k\bar{\theta}\} \quad \text{on} \quad \partial S_{R_1}, \tag{2.5}$$

$$\frac{\partial \bar{u}}{\partial \bar{\nu}} = -\frac{\partial \bar{u}}{\partial \bar{r}} \approx \bar{p}_0 + \sum_{k=1}^{N} \{\bar{p}_k \cos k\bar{\theta} + \bar{q}_k \sin k\bar{\theta}\} \quad \text{on} \quad \partial S_{R_1}, \tag{2.6}$$

where $\bar{a}_k$, $\bar{b}_k$, $\bar{p}_k$ and $\bar{q}_k$ are coefficients, and ν and $\bar{\nu}$ are the outer normals of ∂S_R and ∂S_{R_1}, respectively. In (2.3)-(2.6), (r, θ) and $(\bar{r}, \bar{\theta})$ are two systems of polar coordinates of S_R and S_{R_1} with origins $(0, 0)$ and (x_1, y_1), respectively.

Denote two nodes, $\mathbf{x} = Q = (x, y) = (\rho, \theta)$ and $\mathbf{y} = P = (\xi, \eta) = (r, \phi)$, where $x = \rho\cos\theta, y = \rho\sin\theta, \xi = R\cos\phi$ and $\eta = R\sin\phi$. Then $\rho = \sqrt{x^2 + y^2}$ and $r = \sqrt{\xi^2 + \eta^2}$. The fundamental solutions (FS) of Laplace's equation are given by $\ln|\overline{PQ}| = \ln\sqrt{\rho^2 - 2\rho R\cos(\theta - \phi) + R^2}$. Based on the Green representation formulas [1], there exist different field equations,

$$\int_{\partial S}\left\{\ln|PQ|\frac{\partial u(\mathbf{y})}{\partial \nu_{\mathbf{y}}} - u(\mathbf{y})\frac{\partial \ln|PQ|}{\partial \nu_{\mathbf{y}}}\right\} d\sigma_{\mathbf{y}} = \begin{cases} -2\pi u(Q), & Q \in S, \\ -\pi u(Q), & Q \in \partial S, \\ 0, & \text{otherwise}, \end{cases} \tag{2.7}$$

where $P(\mathbf{y}) \in (S \cup \partial S)$, and $Q(\mathbf{x})$ are the field nodes (or simply nodes) in three different locations. The series expansions of the FS are given by (see [7]),

$$\begin{aligned} \ln|PQ| &= \ln|P(\mathbf{y}) - Q(\mathbf{x})| = \ln|P(r,\phi) - Q(\rho,\theta)| \\ &= U(\mathbf{x},\mathbf{y}) = \begin{cases} U^i(\mathbf{x},\mathbf{y}) = \ln r - \displaystyle\sum_{n=1}^{\infty}\frac{1}{n}(\frac{\rho}{r})^n\cos n(\theta-\phi), & \rho < r, \\ U^e(\mathbf{x},\mathbf{y}) = \ln \rho - \displaystyle\sum_{n=1}^{\infty}\frac{1}{n}(\frac{r}{\rho})^n\cos n(\theta-\phi), & \rho > r, \end{cases} \end{aligned} \tag{2.8}$$

where $\mathbf{x} = (\rho, \theta)$, $\mathbf{y} = (r, \phi)$, and the superscripts "e" and "i" designate the exterior and the interior field nodes $\mathbf{x}$, respectively. Based on the third equation of (2.7), the first kind NFM can be derived from

$$\int_{\partial S_R \cup \partial S_{R_1}} U(\mathbf{x},\mathbf{y})\frac{\partial u(\mathbf{y})}{\partial \nu_{\mathbf{y}}} d\sigma_{\mathbf{y}} = \int_{\partial S_R \cup \partial S_{R_1}} u(\mathbf{y})\frac{\partial U(\mathbf{x},\mathbf{y})}{\partial \nu_{\mathbf{y}}} d\sigma_{\mathbf{y}}, \quad \mathbf{x} \in \bar{S}^c, \tag{2.9}$$

where expansions (2.8) are used, and $\bar{S}^c$ is the complementary domain of $S \cup \partial S$.

First, consider the exterior field nodes $\mathbf{x} = (\rho, \theta)$ with $\rho > r = R$. The explicit algebraic equations of the first kind NFM for the exterior field nodes are obtained in [14], as

$$\begin{aligned} \mathcal{L}_{ext}(\rho,\theta;\bar{\rho},\bar{\theta}) &= -\frac{1}{2}\sum_{k=1}^{M}(\frac{R}{\rho})^k(a_k\cos k\theta + b_k\sin k\theta) \\ &+\frac{1}{2}\sum_{k=1}^{N}(\frac{R_1}{\bar{\rho}})^k(\bar{a}_k\cos k\bar{\theta} + \bar{b}_k\sin k\bar{\theta}) \\ &-\Big\{R(\ln\rho)p_0 - \frac{R}{2}\sum_{k=1}^{M}\frac{1}{k}(\frac{R}{\rho})^k(p_k\cos k\theta + q_k\sin k\theta) \\ &+R_1(\ln\bar{\rho})\bar{p}_0 - \frac{R_1}{2}\sum_{k=1}^{N}\frac{1}{k}(\frac{R_1}{\bar{\rho}})^k(\bar{p}_k\cos k\bar{\theta} + \bar{q}_k\sin k\bar{\theta})\Big\} = 0. \end{aligned} \tag{2.10}$$

Next, consider the exterior field nodes $\mathbf{x} = (\bar\rho, \bar\theta)$ with $\bar\rho < \bar r = R_1$. The other explicit algebraic equations of the first kind NFM are obtained in [14], as

$$\mathcal{L}_{int}(\rho,\theta;\bar\rho,\bar\theta) = -\bar a_0 - \frac{1}{2}\sum_{k=1}^{N}(\frac{\bar\rho}{R_1})^k(\bar a_k\cos k\bar\theta + \bar b_k \sin k\bar\theta) \tag{2.11}$$
$$+a_0 + \frac{1}{2}\sum_{k=1}^{M}(\frac{\rho}{R})^k(a_k\cos k\theta + b_k\sin k\theta)$$
$$-\Big\{R_1(\ln R_1)\bar p_0 - \frac{R_1}{2}\sum_{k=1}^{N}\frac{1}{k}(\frac{\bar\rho}{R_1})^k(\bar p_k\cos k\bar\theta + \bar q_k\sin k\bar\theta)$$
$$+R(\ln R)p_0 - \frac{R}{2}\sum_{k=1}^{M}\frac{1}{k}(\frac{\rho}{R})^k(p_k\cos k\theta + q_k\sin k\theta)\Big\} = 0,$$

where the common factor 2π are canceled. By the first equation with $Q \in S$ of the Green formula (2.7) as used in the boundary element methods (BEM), the solution at the interior field nodes, $\mathbf{x} = (\rho,\theta) \in S$, is expressed by

$$u(\mathbf{x}) = u(\rho,\theta) \tag{2.12}$$
$$= -\frac{1}{2\pi}\int_{\partial S_R \cup \partial S_{R_1}}\Big\{U(\mathbf{x},\mathbf{y})\frac{\partial u(\mathbf{y})}{\partial r} - u(\mathbf{y})\frac{\partial U(\mathbf{x},\mathbf{y})}{\partial r}\Big\}\, d\sigma_{\mathbf{y}}, \quad \mathbf{x} \in S.$$

Then the explicit solution in S is also given in [14] as

$$u_{M-N} = u_{M-N}(\rho,\theta;\bar\rho,\bar\theta) = a_0 - R(\ln R)p_0 - R_1(\ln\bar\rho)\bar p_0 \tag{2.13}$$
$$+\frac{1}{2}\sum_{k=1}^{M}(\frac{\rho}{R})^k(a_k\cos k\theta + b_k\sin k\theta) + \frac{1}{2}\sum_{k=1}^{N}(\frac{R_1}{\bar\rho})^k(\bar a_k\cos k\bar\theta + \bar b_k\sin k\bar\theta)$$
$$+\frac{R}{2}\sum_{k=1}^{M}\frac{1}{k}(\frac{\rho}{R})^k(p_k\cos k\theta + q_k\sin k\theta)$$
$$+\frac{R_1}{2}\sum_{k=1}^{N}\frac{1}{k}(\frac{R_1}{\bar\rho})^k(\bar p_k\cos k\bar\theta + \bar q_k\sin k\bar\theta), \quad (r,\theta) \in S.$$

Explicit formulas (2.10) and (2.11) are derived directly from (2.9) by means of the expansions (2.3)-(2.6) and (2.8). Equations (2.10), (2.11) and (2.13) are called the explicit field (i.e., algebraic) equations of the first kind NFM. In this paper, only Dirichlet problems are confined, where the coefficients, a_k, b_k, $\bar a_k$ and $\bar b_k$, in (2.3) and (2.5) are given. Once the unknown coefficients, p_k, q_k, $\bar p_k$ and $\bar q_k$, have been obtained from (2.10) and (2.11), the interior solutions are provided by (2.13).

2.2. **The Second Kind NFM.** The normal derivatives of the Green formulas (2.9) are given by

$$\frac{\partial}{\partial\nu_{\mathbf{x}}}\Big\{\int_{\partial S_R \cup \partial S_{R_1}} U(\mathbf{x},\mathbf{y})\frac{\partial u(\mathbf{y})}{\partial\nu_{\mathbf{y}}}\, d\sigma_{\mathbf{y}} \tag{2.14}$$
$$-\int_{\partial S_R \cup \partial S_{R_1}} u(\mathbf{y})\frac{\partial U(\mathbf{x},\mathbf{y})}{\partial\nu_{\mathbf{y}}}\, d\sigma_{\mathbf{y}}\Big\} = 0, \quad \mathbf{x} \in \bar S^c,$$

where $\frac{\partial}{\partial\nu_{\mathbf{x}}} = \frac{\partial}{\partial\rho}$ for $\rho > R$ and $\frac{\partial}{\partial\nu_{\mathbf{x}}} = -\frac{\partial}{\partial\bar\rho}$ for $\bar\rho < R_1$. Based on (2.14), the second kind NFM is developed in [10], where two explicit algebraic equations for exterior field nodes are provided as

$$\begin{aligned}(2.15)\quad \mathcal{D}_{ext}(\rho,\theta;\bar{\rho},\bar{\theta}) &= \frac{\partial}{\partial\rho}\mathcal{L}_{ext}(\rho,\theta;\bar{\rho},\bar{\theta}) = \frac{1}{2}\sum_{k=1}^{M} k(\frac{R^k}{\rho^{k+1}})(a_k\cos k\theta + b_k\sin k\theta) \\ &-\frac{1}{2}\sum_{k=1}^{N} k(\frac{R_1^k}{\bar{\rho}^{k+1}})\Big(\bar{a}_k\cos((k+1)\bar{\theta}-\theta) + \bar{b}_k\sin((k+1)\bar{\theta}-\theta)\Big) \\ &-\Bigg\{(\frac{R}{\rho})p_0 + \frac{1}{2}\sum_{k=1}^{M}(\frac{R}{\rho})^{k+1}(p_k\cos k\theta + q_k\sin k\theta) + (\frac{R_1}{\bar{\rho}})\bar{p}_0\cos(\theta-\bar{\theta}) \\ &+\frac{1}{2}\sum_{k=1}^{N}(\frac{R_1}{\bar{\rho}})^{k+1}\Big(\bar{p}_k\cos((k+1)\bar{\theta}-\theta) + \bar{q}_k\sin((k+1)\bar{\theta}-\theta)\Big)\Bigg\} = 0,\end{aligned}$$

and

$$\begin{aligned}(2.16)\qquad \mathcal{D}_{int}(\rho,\theta;\bar{\rho},\bar{\theta}) &= -\frac{\partial}{\partial\bar{\nu}}\mathcal{L}_{int}(\rho,\theta;\bar{\rho},\bar{\theta}) = \frac{\partial}{\partial\bar{\rho}}\mathcal{L}_{int}(\rho,\theta;\bar{\rho},\bar{\theta}) \\ &= -\frac{1}{2}\sum_{k=1}^{N} k(\frac{\bar{\rho}^{k-1}}{R_1^k})(\bar{a}_k\cos k\bar{\theta} + \bar{b}_k\sin k\bar{\theta}) \\ &+\frac{1}{2}\sum_{k=1}^{M} k(\frac{\rho^{k-1}}{R^k})\Big(a_k\cos((k-1)\theta+\bar{\theta}) + b_k\sin((k-1)\theta+\bar{\theta})\Big) \\ &+\frac{1}{2}\sum_{k=1}^{N}(\frac{\bar{\rho}}{R_1})^{k-1}(\bar{p}_k\cos k\bar{\theta} + \bar{q}_k\sin k\bar{\theta}) \\ &+\frac{1}{2}\sum_{k=1}^{M}(\frac{\rho}{R})^{k-1}\Big(p_k\cos((k-1)\theta+\bar{\theta}) + q_k\sin((k-1)\theta+\bar{\theta})\Big) = 0.\end{aligned}$$

Although Eqs. (2.10), (2.11), (2.15) and (2.16) are derived from (2.9) and (2.14), where the nodes Q are located outside of S, they are still valid for the nodes on the domain boundary, $Q \in \partial S$, under a certain smoothness of the solutions (e.g., $u \in H^3(\partial S) \wedge u_\nu \in H^2(\partial S)$). Although Eq. (2.13) is derived from (2.12), where the nodes Q are inside of S, the solutions of (2.13) and their normal derivatives are still valid for the nodes $Q \in \partial S$, under the same smoothness of the solutions. A strict analysis is explored in [14, 10]. Since the solutions (2.13) are harmonic functions to satisfy Laplace's equation already, the unique solutions of Dirichlet problems can be obtained directly by satisfying (2.3) & (2.5). Under a consistent condition, however, the solutions of Neumann problems by satisfying (2.4) & (2.6) are existent and solvable, see [10]. Such algorithms are called the interior field method (IFM) of the first and the second kinds, respectively. It is proved in [8, 10] that the IFM is the special case of the NFM at $Q \in \partial S$. From computed results and theoretical analysis, the stability of the NFM is optimal among all nodes used in the NFM. Hence, the NFM is replaced by the IFM in many applications, see [8, 9, 11, 10, 14].

2.3. **Dual Null Field Methods.** Traditionally, the first and the second kinds of the NFM are used for the Dirichlet and Neumann problems, respectively, see [14, 10]. The first kind NFM may also be applied to Neumann problems, where Eqs. (2.4) and (2.6) are given with known coefficients $p_k, q_k, \bar{p}_k$ and q_k, but the coefficients $a_k, b_k, \bar{a}_k$ and $\bar{b}_k$ are sought. The numerical performance is as good as that by the second kind NFM, see [10]. Hence, we may also apply (2.15) and (2.16) of the second kind NFM for Dirichlet problems, where the coefficients $a_k, b_k, \bar{a}_k$ and $\bar{b}_k$ are given, but the coefficients $p_k, q_k, \bar{p}_k$ and q_k are sought. When two kinds of NFMs are applied for exterior and interior boundaries, there are four types, I-I, II-II, I-II and II-I, where I and II denote the first and the second kind NFMs, respectively, and their appearances before and behind from "-" denote the exterior and the interior boundaries, respectively.

First, consider (2.10) and (2.11) of the first kind NFM in [14] for the exterior and the interior boundaries, respectively,

$$I - I := \begin{pmatrix} R\ln\rho & R_1\ln\bar{\rho} \\ R\ln R & R_1\ln R_1 \end{pmatrix} \begin{pmatrix} p_0 \\ \bar{p}_0 \end{pmatrix} + \begin{pmatrix} f_0 \\ \bar{f}_0 \end{pmatrix} = \vec{0}, \tag{2.17}$$

where f_0 and $\bar{f}_0$ are the rest parts of algebraic equations without p_0 and $\bar{p}_0$. The algorithm singularity occurs from degenerate scales, if and only if the zero determinant of the matrix of the leading coefficients p_0 and $\bar{p}_0$ in (2.17). For type I-I, the singularity happens when $\rho = R = 1$, which is an important case of degenerate scales in applications, called Degenerate Case I in [11]. A complete analysis of algorithm singularity is explored in [11], to discover a new Degenerate Case III called.

For Dirichlet problems, we may use both of the second kind NFM for the exterior and the interior boundaries, respectively, and obtain from (2.15) and (2.16),

$$II - II := \begin{pmatrix} \frac{R}{\rho} & \frac{R_1}{\bar{\rho}}\cos(\theta - \bar{\theta}) \\ 0 & 0 \end{pmatrix} \begin{pmatrix} p_0 \\ \bar{p}_0 \end{pmatrix} + \begin{pmatrix} f_0 \\ \bar{f}_0 \end{pmatrix} = \vec{0}. \tag{2.18}$$

Next, we also use the first and second kinds of NFM for the exterior and interior circular boundaries, respectively, and obtain from (2.10) and (2.16),

$$I - II := \begin{pmatrix} R\ln\rho & R_1\ln\bar{\rho} \\ 0 & 0 \end{pmatrix} \begin{pmatrix} p_0 \\ \bar{p}_0 \end{pmatrix} + \begin{pmatrix} f_0 \\ \bar{f}_0 \end{pmatrix} = \vec{0}. \tag{2.19}$$

For types II-II and I-II, the singularity always happens. Hence, the second kind NFM can not be used for the interior boundary of Dirichlet problems.

Lastly, let us apply the second and first kinds of NFM for the exterior and interior circular boundaries, respectively, and obtain from (2.15) and (2.11),

$$II - I := \begin{pmatrix} \frac{R}{\rho} & \frac{R_1}{\bar{\rho}}\cos(\theta - \bar{\theta}) \\ R\ln R & R_1\ln R_1 \end{pmatrix} \begin{pmatrix} p_0 \\ \bar{p}_0 \end{pmatrix} + \begin{pmatrix} f_0 \\ \bar{f}_0 \end{pmatrix} = \vec{0}. \tag{2.20}$$

From the analysis in the next section, type II-I is effective to overcome degenerate scales. This kind combination of two kinds of the NFM is called the dual NFM (denoted as the DNFM) in this paper. The numerical solutions can be obtained easily by using the Gaussian elimination or iteration methods. More importantly, the optimal stability and optimal convergence rates can be reached, and given in Section 4. Note that these approaches are analogous to deal with the mixed problems by the NFM in [21]. The theoretical analysis and numerical performance of Type II-I in (2.20) are the goals of this paper.

For the DNFM, Eqs. (2.15) and (2.11) are denoted simply as

$$\mathcal{D}_{ext}(\rho, \theta; \bar{\rho}, \bar{\theta}) = 0, \quad on \;\; \partial S_R, \tag{2.21}$$

$$\mathcal{L}_{int}(\rho, \theta; \bar{\rho}, \bar{\theta}) = 0 \quad on \;\; \partial S_{R_1}. \tag{2.22}$$

For better stability, the field nodes (ρ, θ) are confined on the same circle, i.e., $\rho = constant$, based on the analysis in [11]. We may choose $2(M+N)+2$ collocation equations uniformly located on the exterior and the interior circles, $\rho = R+\epsilon \geq R$ and $\bar{\rho} = R_1 - \bar{\epsilon}$. For (2.21) and (2.22), the collocation equations are given by

$$\frac{1}{M}\mathcal{D}_{ext}(R+\epsilon, jh; \bar{\rho}_j, \bar{\theta}_j) = \frac{1}{M} f(jh), \quad j = 0, 1, ..., 2M, \tag{2.23}$$

$$\mathcal{L}_{int}(\rho_j, \theta_j; R_1 - \bar{\epsilon}, j\bar{h}) = g(j\bar{h}), \quad j = 0, 1, ..., 2N, \tag{2.24}$$

where $\epsilon \geq 0, \bar{\epsilon} \in [0, R_1)$, $h = \frac{2\pi}{2M+1}$ and $\bar{h} = \frac{2\pi}{2N+1}$. The factor $\frac{1}{M}$ is used in (2.23) for optimal convergence rates, based on the mixed Dirichlet and the Neumann conditions in [12, 15, 16]. The corresponding polar coordinates (ρ_j, θ_j) and $(\bar{\rho}_j, \bar{\theta}_j)$ in (2.23) and (2.24) can be evaluated from $(R_1 - \bar{\epsilon}, j\bar{h})$ and $(R+\epsilon, jh)$, based on (2.1) and (2.2). Eqs. (2.23) and (2.24) are denoted as the following linear algebraic equations,

$$\mathbf{A}\mathbf{x} = \mathbf{b}, \tag{2.25}$$

where the matrix $\mathbf{A} \in \mathbf{R}^{n \times n}$, the unknown vector $\mathbf{x}$ $(\in \mathbf{R}^n) = \{p_k, q_k, \bar{p}_k, \bar{q}_k\}^T$ and $n = 2(M+N+1)$. The unknown coefficients in $\mathbf{x}$ can be solved from (2.25) directly, if the matrix $\mathbf{A}$ is nonsingular. Once all the coefficients are known, the explicit solutions in S are given in (2.13).

2.4. **Derivatives of the First Kind NFM along Other Directions.** The type II-I of the dual techniques implies that the hypersingularity is applied to the exterior circular boundary. Can we find other kinds of dual techniques? The second kind NFM is derived based on (2.14), where $\frac{\partial}{\partial \nu_{\mathbf{x}}}$ are the derivatives along the radial direction $\nu_{\mathbf{x}}$. In fact, we may have other directional derivatives $\frac{\partial}{\partial \ell_{\mathbf{x}}}$, denoted as

$$\begin{aligned} \frac{\partial}{\partial \ell_{\mathbf{x}}}\Big\{ \int_{\partial S_R \cup \partial S_{R_1}} & U(\mathbf{x},\mathbf{y}) \frac{\partial u(\mathbf{y})}{\partial \nu_{\mathbf{y}}}\, d\sigma_{\mathbf{y}} \\ - \int_{\partial S_R \cup \partial S_{R_1}} & u(\mathbf{y}) \frac{\partial U(\mathbf{x},\mathbf{y})}{\partial \nu_{\mathbf{y}}}\, d\sigma_{\mathbf{y}} \Big\} = 0, \quad \mathbf{x} \in \bar{S}^c, \end{aligned} \tag{2.26}$$

where $\ell_{\mathbf{x}}$ is any direction in $\mathbf{x}$. Since only the degenerate scales are our concern, we derive the algebraic equations only related to the leading coefficients of p_0 and $\bar{p}_0$ from (2.26). By following [10], we have from (2.15)

$$\frac{\partial}{\partial \ell}\{-R(\ln \rho)p_0 - R_1(\ln \bar{\rho})\bar{p}_0)\} = -R\frac{p_0}{\rho}\cos(\ell, \rho) - R_1\frac{\bar{p}_0}{\bar{\rho}}\cos(\ell, \bar{\rho}). \tag{2.27}$$

Denote the angle ξ of ℓ from x axis, there exist the equalities,

$$\cos(\ell, \rho) = \cos(\theta - \xi), \quad \cos(\ell, \bar{\rho}) = \cos(\bar{\theta} - \xi). \tag{2.28}$$

The leading coefficients p_0 and $\bar{p}_0$ in (2.15) are modified from (2.27) as

$$R\frac{p_0}{\rho}\cos(\theta - \xi) + R_1\frac{\bar{p}_0}{\bar{\rho}}\cos(\bar{\theta} - \xi). \tag{2.29}$$

Other dual techniques may be designed, where $\frac{\partial}{\partial \ell_{\mathbf{x}}}\mathcal{L}_{ext} = 0$ and $\mathcal{L}_{int} = 0$ are used for the exterior and the interior boundaries, respectively. Then Eqs. (2.20) are modified, as

$$II^* - I := \begin{pmatrix} \frac{R}{\rho}\cos(\theta - \xi) & \frac{R_1}{\bar{\rho}}\cos(\bar{\theta} - \xi) \\ R\ln R & R_1 \ln R_1 \end{pmatrix} \begin{pmatrix} p_0 \\ \bar{p}_0 \end{pmatrix} + \begin{pmatrix} f_0^* \\ \bar{f}_0 \end{pmatrix} = \vec{0}. \tag{2.30}$$

When ℓ is along the radial direction $\nu_{\mathbf{x}}$, we have $\xi = \theta$, Eqs. (2.30) lead to (2.20). When ℓ is along the radian direction θ, we have $\xi = \theta + \frac{\pi}{2}$ and $\cos(\theta - \xi) = \cos(\frac{\pi}{2}) = 0$. Eqs (2.30) lead to

$$(2.31) \qquad II^* - I := \begin{pmatrix} 0 & \frac{R_1}{\bar\rho}\sin(\theta - \bar\theta) \\ R\ln R & R_1 \ln R_1 \end{pmatrix} \begin{pmatrix} p_0 \\ \bar p_0 \end{pmatrix} + \begin{pmatrix} f_0^* \\ \bar f_0 \end{pmatrix} = \vec{0}.$$

The zero determinant of matrix of leading coefficients in (2.31) occurs,

$$(2.32) \qquad Det(II^* - I) = -\frac{RR_1}{\bar\rho}(\ln R)\sin(\theta - \bar\theta) = 0,$$

provided that $R = 1$. Hence, type $II^* - I$ of dual techniques fails to overcome Degenerate Case I, if ℓ is along the radian direction θ. For the general dual techniques with $\xi \neq \theta$ but $\xi \neq \theta + \frac{\pi}{2}$, by following similar arguments above, we may prove the non-singularity of the coefficient matrix in (2.30), to also bypass the degenerate scales. However, the corresponding algorithms are more complicated, so that they are not effective for real applications, compared with (2.20). We write this conclusion as a proposition.

Proposition 2.1. *The general dual techniques (2.30) fail to overcome the Degenerate Case I, if ℓ is along the radian direction θ. The algorithms of the dual techniques (2.20) of type II-I are the simplest among (2.30), if ℓ is not along the radian direction θ.*

We may solicit higher order derivatives on the NFM for the exterior boundary conditions, to have

$$(2.33) \qquad \frac{\partial^k}{\partial(\nu_{\mathbf{x}})^k}\Big\{\int_{\partial S_R \cup \partial S_{R_1}} U(\mathbf{x},\mathbf{y})\frac{\partial u(\mathbf{y})}{\partial \nu_{\mathbf{y}}}\, d\sigma_{\mathbf{y}} - \int_{\partial S_R \cup \partial S_{R_1}} u(\mathbf{y})\frac{\partial U(\mathbf{x},\mathbf{y})}{\partial \nu_{\mathbf{y}}}\, d\sigma_{\mathbf{y}}\Big\} = 0, \mathbf{x} \in \bar S^c,$$

where $k \geq 1$. When Eq. (2.33) is used for the exterior boundary, the degenerate scales can also be removed. However, they are not recommended, since the corresponding algorithms are much more complicated, and since higher supper-singularity is involved wherein.

3. Analysis on Degenerate Scales for the DNFM

The discrete form from (2.20) of type II-I is denoted as

$$(3.1) \qquad \frac{R}{\rho_j}p_0 + \frac{R_1}{\bar\rho_j}\cos(\theta_j - \bar\theta_j)\bar p_0 + f_0(\rho_j, \theta_j; a_k, b_k, ..., \bar q_k) = 0, \quad j = 0, 1, ..., 2M,$$

$$(3.2) \qquad R(\ln R)p_0 + R_1(\ln R_1)\bar p_0 + \bar f_0(\bar\rho_j^*, \bar\theta_j^*; a_k, b_k, ..., \bar q_k) = 0, \quad j = 0, 1, ..., 2N,$$

where $P(\rho_j, \theta_j) = P(\bar\rho_j, \bar\theta_j)$. In fact, Equations (3.1) and (3.2) are the discrete forms of (2.23) and (2.24). For simplicity in analysis, the factors $\frac{1}{M}$ in (2.23) are omitted, since they do not affect on the matrix singularity. Denote the matrix and vectors related to p_0 and $\bar{p}_0$ of (3.1) and (3.2) as

$$\mathbf{T_{deg}}\mathbf{y} = \begin{pmatrix} \frac{R}{\rho_0} & \frac{R_1}{\bar{\rho}_0}\cos(\theta_0-\bar{\theta}_0) \\ \frac{R}{\rho_1} & \frac{R_1}{\bar{\rho}_1}\cos(\theta_1-\bar{\theta}_1) \\ \cdots & \cdots \\ \frac{R}{\rho_{2M}} & \frac{R_1}{\bar{\rho}_{2M}}\cos(\theta_{2M}-\bar{\theta}_{2M}) \\ & \\ R\ln R & R_1\ln R_1 \\ R\ln R & R_1\ln R_1 \\ \cdots & \cdots \\ R\ln R & R_1\ln R_1 \end{pmatrix} \begin{pmatrix} p_0 \\ \bar{p}_0 \end{pmatrix}, \tag{3.3}$$

where $\mathbf{y} = (p_0, \bar{p}_0)^T$, and the matrix $\mathbf{T_{deg}} \in R^{n\times 2}$ with $n = 2(M+N+1)$. The algorithm singularity of degenerate scales is defined in [11], provided that the constants p_0 and $\bar{p}_0$ can not be determined uniquely from (3.1) and (3.2), which is equivalent to the deficiency of matrix $\mathbf{T_{deg}}$

$$\mathrm{rank}(\mathbf{T_{deg}}) \le 1. \tag{3.4}$$

Equation (3.4) indicates that two column vectors of $\mathbf{T_{deg}}$ are parallel to each other, thus causing a singularity of the discrete matrix of (3.1) and (3.2). If $\mathrm{rank}(\mathbf{T_{deg}}) = 1$, all exterior nodes are called pitfall nodes of degenerate scales, and there occurs a singularity of matrix $\mathbf{A}$ in (2.25), see [11].

3.1. **Basic Theorem.** First, we study the usual collocation nodes, where exterior field nodes are all located on the same circle: $\rho \ge R$ and $\rho = constant$ in (2.23). We have the following theorem.

Theorem 3.1. *Suppose that the second and the first kinds of NFM (i.e., (2.15) and (2.11)) are used for the exterior and the interior circular boundaries, respectively. For $\rho = R+\epsilon$ with constant $\epsilon \ge 0$ and $M \ge 1$ in (3.1), there does not exist the algorithm singularity from degenerate scales.*

Proof. The algorithm singularity from degenerate scales occurs if and only if only the zero determinant of the leading coefficients p_0 and $\bar{p}_0$ of (2.20) occurs,

$$Det(II-I) = RR_1\{\frac{\ln R_1}{\rho} - \frac{\ln R}{\bar{\rho}}\cos(\theta-\bar{\theta})\} = 0, \tag{3.5}$$

where $R > R_1 > 0$, $\rho > 0$ and $\bar{\rho} > 0$. Eq. (3.5) leads to

$$\bar{\rho}\ln R_1 = \rho(\ln R)\cos(\theta-\bar{\theta}). \tag{3.6}$$

Without loss of generality, let (ρ,θ) and $(\bar{\rho},\bar{\theta})$ be two polar coordinate systems at $O(0,0)$ and $\bar{O}(-a,0)$ with $a \ge 0$, respectively, see Figure 1. First, for the concentric boundaries, ∂S_R and ∂S_{R_1} have the same origin $(0,0)$ (i.e., $a=0$). Then we have $\bar{\rho} = \rho$ and $\theta = \bar{\theta}$. Eq. (3.6) leads to

$$\rho\ln R_1 = \rho\ln R, \tag{3.7}$$

which is impossible since $R_1 < R$. This implies that there does not exist any degenerate scale for the concentric boundaries. Next, when $R = 1$, we have $\ln R = 0$ and $\ln R_1 < \ln R = 0$, to confirm the invalidity of (3.6). Note that the exterior boundary with radius $R = 1$ is the important case of degenerate scales in the NFM, called Degenerate Case I in [11], which is removed successfully in the dual type II-I.

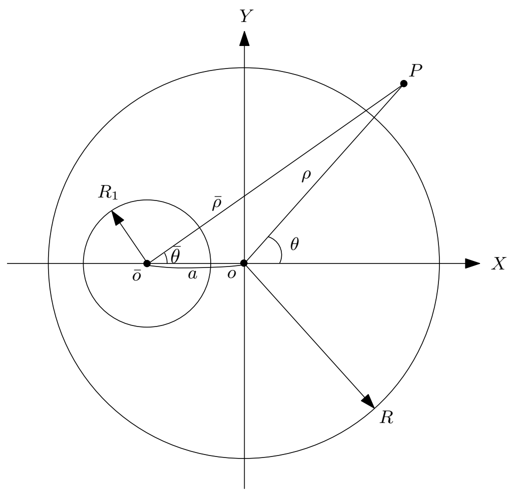

FIG. 1. The distances ρ and $\bar{\rho}$ of the exterior field P to two origins O and $\bar{O}$.

Below, we discuss the eccentric boundaries (i.e., $a \neq 0$) with $R \neq 1$, and seek all nodes to satisfy (3.6), called the pitfall nodes in [11]. Consider the triangle $\triangle OP\bar{O}$ consisting of $O(0,0), P(\rho,\theta)$ and $\bar{O}(-a,0)$, see Figure 1. The distance a between O and $\bar{O}$ is given by

$$a^2 = \rho^2 + \bar{\rho}^2 - 2\rho\bar{\rho}\cos(\theta - \bar{\theta}). \tag{3.8}$$

Then we have

$$\cos(\theta - \bar{\theta}) = \frac{\rho^2 + \bar{\rho}^2 - a^2}{2\rho\bar{\rho}}. \tag{3.9}$$

Combining (3.6) and (3.9) gives

$$2\bar{\rho}^2 \ln R_1 = (\ln R)(\rho^2 + \bar{\rho}^2 - a^2). \tag{3.10}$$

For $R \neq 1$, we have

$$(2\frac{\ln R_1}{\ln R} - 1)\bar{\rho}^2 = \rho^2 - a^2. \tag{3.11}$$

Since $\rho > a$, one root $\bar{\rho}$ of (3.11) is found by

$$\bar{\rho} = \sqrt{\frac{\rho^2 - a^2}{2\frac{\ln R_1}{\ln R} - 1}} = \sqrt{\frac{\rho^2 - a^2}{\mu}}, \tag{3.12}$$

provided that

$$\mu = 2\frac{\ln R_1}{\ln R} - 1 > 0. \tag{3.13}$$

Eq. (3.13) indicates $\mu \neq 1$ since $R_1 < R \neq 1$. From the symmetry, two field nodes $P^+(\bar{\rho},\bar{\theta})$ and $P^-(\bar{\rho},-\bar{\theta})(\bar{\theta} \neq 0,\pi)$ may have the same $\bar{\rho}$ of (3.12). Hence, there exist, at most, two field nodes to satisfy (3.5). When $M \geq 1$, the number of collocation equations in (3.1) is $2M+1 \geq 3$. When $\rho = constant$, there are, at least, two different values $\bar{\rho}$ of nodes from (2.2). Then not all pars $[\rho,\bar{\rho}]$ can satisfy (3.11), so that the left two column vectors from (3.3) are linearly independent to each other.

Hence $\mathrm{rank}(\mathbf{T_{deg}}) = 2$, and the discrete matrices from leading coefficients p_0 and $\bar{p}_0$ are nonsingular, thus to remove the degenerate scales. This completes the proof of Theorem 3.1. □

Based on Theorem 3.1, for $\rho = constant$, all degenerate scales, including Degenerate Case I, can be bypassed, when $M \geq 1$ in (2.23). This is significant, compared with the singularity of the NFM (i.e., type I-I) at $\rho = R = 1$, called Degenerate Case I in [11].

3.2. **Degenerate Case IIIA.** Theorem 3.1 confirms no degenerate scales under condition $\rho = constant$. It is challenging to seek all kinds of degenerate scales of the dual techniques, as done in [11] for the NFM. In this subsection, we assume $\rho \geq R$, but do not confine $\rho = constant$. To this end, let us first study condition (3.13) more in detail. Since $R = 1$ is excluded in pitfall nodes, there exist only two cases from (3.13),

$$2\ln R_1 < \ln R \quad \text{for } R < 1, \quad \text{called Case III}, \tag{3.14}$$

$$2\ln R_1 > \ln R \ (i.e., R_1^2 > R) \quad \text{for } R > 1, \quad \text{called Case IVA}. \tag{3.15}$$

Since $R_1^2 < R_1 R < R$ for $R < 1$, Eq. (3.14) holds. Case III for $R_1 < R < 1$ and Case IV for $1 < R_1 < R$ are called in [11, p.163]. Since Eq. (3.15) is a special of Case IV under condition, $R_1^2 > R > 1$, and then called Case IVA in this paper. Therefore, there may have the solution $\bar{\rho}$ from (3.12), under $R < 1$ or $R_1^2 > R > 1$. Otherwise, no solution of (3.11) exists. From (2.2), for the one $\bar{\rho}$, at most, two field nodes (ρ, θ) and $(\rho, -\theta)$ may be found. We may follow the analytic outlines in [11, Section 3.3], to find all pitfall nodes to satisfy (3.5). The pitfall nodes are defined by the nodes $(\bar{\rho}, \bar{\theta}^{\pm})$ of (3.12) to satisfy the conditions of the solution region Ω_R of nodes $P(\rho, \bar{\rho})$ (see Figure 2)

$$\rho - a \leq \bar{\rho} \leq \rho + a, \quad \rho \geq R, \tag{3.16}$$

which is given in [11, Lemma 3.1].

Below, we will consider the general choices of the exterior nodes $\rho \geq R$, which are not confined on the same circle as those in (2.23). We choose

$$\frac{\sqrt{h}}{M}\mathcal{D}_{ext}(R + \epsilon_j, \theta_j; \bar{\rho}_j, \bar{\theta}_j) = \frac{\sqrt{h}}{M} f_0(\theta_j), \quad j = 0, 1, ..., 2M, \tag{3.17}$$

to replace (2.23), where $\epsilon_j (\geq 0)$ are not constant, and $0 \leq \theta_j < \theta_{j+1} < 2\pi$. A similar model to the degenerate Case III in [11] can be found for $R < 1$, but under more a specific limitation of R, R_1 and a, given in Lemma 3.2 below.

Lemma 3.1. *There does not exist any pitfall node for Case IVA of (3.15), but may exist pitfall nodes for Case III of (3.14).*

Proof. We have from (3.11) and (3.16)

$$\mu(\rho - a)^2 \leq \rho^2 - a^2 \leq \mu(\rho + a)^2, \tag{3.18}$$

where μ is given in (3.13). Eqs. (3.18) lead to

$$\mu(\rho - a) \leq \rho + a, \quad \rho - a \leq \mu(\rho + a). \tag{3.19}$$

Then we have

$$(\mu - 1)\rho \leq (\mu + 1)a, \quad -(1 + \mu)a \leq (\mu - 1)\rho, \tag{3.20}$$

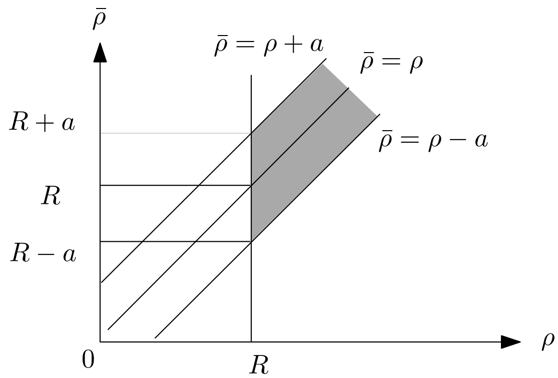

FIG. 2. The solution region Ω_R of $P(\rho, \bar{\rho})$ with $\rho \geq R$ and $\rho - a \leq \bar{\rho} \leq \rho + a$.

to give

$$-\frac{\mu+1}{\mu-1}a \leq \rho \leq \frac{\mu+1}{\mu-1}a, \quad \mu \neq 1, \tag{3.21}$$

where the ratio in front of a is given from μ in (3.13)

$$\frac{\mu+1}{\mu-1} = \frac{2\frac{\ln R_1}{\ln R} - 1 + 1}{2\frac{\ln R_1}{\ln R} - 1 - 1} = \frac{\ln R_1}{\ln R_1 - \ln R} = \frac{\ln R_1}{\ln \frac{R_1}{R}}. \tag{3.22}$$

Since $\rho \geq a$ we have from the right hand of (3.21)

$$a \leq \rho \leq \frac{\mu+1}{\mu-1}a, \tag{3.23}$$

to give from (3.22)

$$1 \leq \frac{\mu+1}{\mu-1} = \frac{\ln R_1}{\ln \frac{R_1}{R}}. \tag{3.24}$$

Since $R_1 < R$ and $\ln \frac{R_1}{R} < 0$, there must be $\ln R_1 < 0$ and $R_1 < 1$, based on (3.24). In this case, multiplying $\ln \frac{R_1}{R} (< 0)$ to both sides of (3.24) leads to

$$\ln R_1 - \ln R = \ln \frac{R_1}{R} \geq \ln R_1, \tag{3.25}$$

and then

$$\ln R < 0, \quad R < 1. \tag{3.26}$$

This implies Case III of (3.14) for possible pitfall nodes.

Next, for Case IVA of (3.15), since $R_1^2 > R$, we have $R_1 > 1$, and then

$$\frac{\ln R_1}{\ln \frac{R_1}{R}} < 0, \tag{3.27}$$

which is against (3.24). Hence, Case IVA is excluded in pitfall nodes and degenerate scales. This completes the proof of Lemma 3.1. □

To find the pitfall nodes in Case III of (3.14), we have the following lemma.

Lemma 3.2. *There may exist the pitfall nodes for Case III($R_1 < R < 1$), when the following condition is satisfied,*

$$R \le R_1^{1-\frac{a}{R}} = R^*, \quad 0 < a \le R - R_1. \tag{3.28}$$

Proof. For $R_1 < R < 1$ in Case III, since $\frac{\mu+1}{\mu-1} > 0$ from (3.24), the left side of (3.21) is satisfied automatically. Then only one condition remains from the right side of (3.21), which leads to

$$R \le \rho \le \frac{\mu+1}{\mu-1} a = \frac{\ln R_1}{\ln \frac{R_1}{R}} a, \tag{3.29}$$

where we have added $\rho \ge R$. Eq. (3.29) gives a specific relation among a, R_1 and R,

$$R \le \frac{\ln R_1}{\ln \frac{R_1}{R}} a. \tag{3.30}$$

Eq. (3.30) is rewritten as

$$\frac{\ln \frac{R}{R_1}}{\ln \frac{1}{R_1}} = \frac{\ln \frac{R_1}{R}}{\ln R_1} \le \frac{a}{R}. \tag{3.31}$$

Since $R_1 < R < 1$, we have

$$\ln \frac{R}{R_1} \le \frac{a}{R} \times \ln \frac{1}{R_1} = \ln \frac{1}{(R_1)^{\frac{a}{R}}}. \tag{3.32}$$

Hence, we obtain

$$\frac{R}{R_1} \le \frac{1}{(R_1)^{\frac{a}{R}}}, \tag{3.33}$$

to give the condition for pitfall nodes existing for Case III,

$$R \le R_1^{1-\frac{a}{R}} = R^*, \quad 0 < a \le R - R_1. \tag{3.34}$$

This is the desired result (3.28), and completes the proof of Lemma 3.2. □

Note that for the concentric boundaries, $a = 0$, the condition (3.28) is invalid, due to $R_1 < R$. Denote the function

$$\phi(\tau) = R_1^{1-\tau}, \quad \tau = \frac{a}{R}, \tag{3.35}$$

where $0 < \tau \le 1 - \frac{R_1}{R}$, since $0 < a \le R - R_1$. The derivatives are positive, $\phi'(\tau) = -(\ln R_1) R_1^{1-\tau} > 0$. Hence, to relax the limitation of R by (3.28), we may choose a larger $\tau = \frac{a}{R}$. We do not intend to seek the optimal choice of τ, but rather take $\tau = \frac{1}{2}$ for example. Choose $a = \frac{R}{2}$ and $R < 1$. Then since $R_1 \le \frac{R}{2}$, Condition (3.28) leads to

$$R \le \sqrt{R_1} \le \sqrt{\frac{R}{2}} = R^*. \tag{3.36}$$

From (3.36) we have $R \le 0.5 = R^*$. Hence for $\tau = \frac{1}{2}$, there do not exist degenerate scales for $R > \frac{1}{2}$, different from Degenerate Case III for all $R < 1$ in [11]. Then, a new Degenerate Case IIIA with $R \le R^* < 1$ can be found from the following theorem.

Theorem 3.2. *Suppose that Eqs. (3.17) and (2.24) are used for the exterior and the interior circular boundaries, respectively. For Case III($R_1 < R < 1$) under condition (3.28), there does exist the algorithm singularity from degenerate scales, called Degenerate Scale IIIA.*

Proof. Eq. (3.12) is denoted as a hyperbolic curve of second order,

$$\frac{\rho^2}{a^2} - \frac{\bar\rho^2}{(\frac{a}{\sqrt{\mu}})^2} = 1. \tag{3.37}$$

Since $\rho > 0$ and $\bar\rho > 0$, the function (3.12) is confined to be the hyperbolic curve in the first quarter. Since $R_1 < R < 1$, we have $\frac{\ln R_1}{\ln R} > 1$, to give

$$\mu = 2\frac{\ln R_1}{\ln R} - 1 > 1. \tag{3.38}$$

Hence we have from (3.12)

$$\bar\rho = \sqrt{\frac{\rho^2 - a^2}{\mu}} < \sqrt{\rho^2 - a^2} < \rho. \tag{3.39}$$

Then, the nodes with $\bar\rho = \rho$ are excluded from pitfall nodes. Since the nodes with $\bar\rho = \rho$ are located on the vertical line $x = -\frac{a}{2}$, the pitfall nodes are located only on the left plane with $x < -\frac{a}{2}$. Hence, the contour of pitfall nodes is not a closed curve, different from that for Degenerate Case III in [11, Figures 10 and 11].

Next, we find the contour of all pitfall nodes under condition (3.28). The hyperbolic curve has an asymptotic line in the first quarter with $\rho > 0$ and $\bar\rho > 0$,

$$\bar\rho = \frac{\rho}{\sqrt{\mu}}, \quad \mu > 1. \tag{3.40}$$

Other two lines are given in Figure 2,

$$\bar\rho = \rho - a, \quad \rho = R. \tag{3.41}$$

Since $\mu > 1$, the intersection nodes of three lines in (3.40) and (3.41) formulate a triangle $\triangle ABC$, see Figure 3. Denote the nodes by pars $(\rho, \bar\rho)$. Two vertices of $\triangle ABC$ are on $\rho = R$, and given by $A(R, R-a)$ and $B(R, \frac{R}{\sqrt{\mu}})$. The third vertex of $\triangle ABC$ is found as $C(\rho^*, \frac{\rho^*}{\sqrt{\mu}})$ with $\rho^* = \frac{a}{1-\frac{1}{\sqrt{\mu}}}$. The curve of (3.12) satisfying (3.28) will cross the triangle $\triangle ABC$, to confirm the degenerate scales existing. This cross segment of this curve is denoted by $\widehat{QT}$ in Figure 3, where the left boundary point is denoted by $Q(R, \sqrt{\frac{R^2-a^2}{\mu}})$. From $\mu > 1$ and Lemma 3.2, there exist the bounds,

$$R - a < \sqrt{\frac{R^2 - a^2}{\mu}} < \frac{R}{\sqrt{\mu}}. \tag{3.42}$$

Hence the left boundary point, $Q(R, \sqrt{\frac{R^2-a^2}{\mu}})$, of $\widehat{QT}$ is located within the vertical segment $\overline{AB}$. Since the curve $\widehat{QT}$ of hyperbolic lines can not reach $\overline{BC}$ of the asymptotic line (3.40), the monotonously increasing curve $\widehat{QT}$ must have the right boundary point T on $\overline{AC}$, see Figure 3. If all different $2M+1$ nodes $(\rho, \bar\rho)$ are chosen on the curve $\widehat{QT}$, the singularity occurs for (3.17) and (2.24), called Degenerate Case IIIA. This completes the proof of Theorem 3.2. $\square$

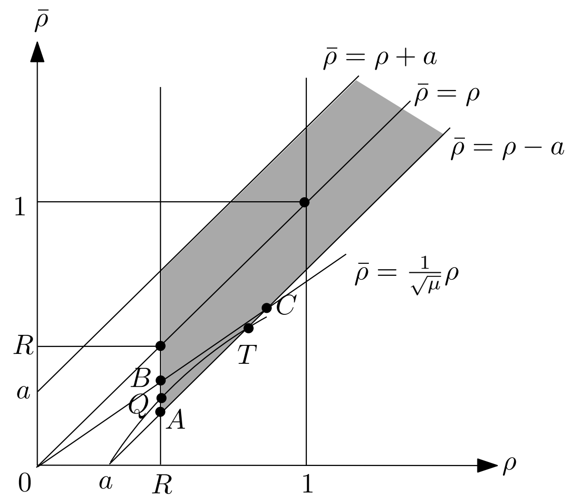

FIG. 3. Pitfall nodes $\in \Omega_R$ of Case IIIA with $R_1 < R < 1$, where $\bar\rho = \sqrt{\frac{\rho^2 - a^2}{\mu}}$ with $\mu > 1$.

3.3. **An Example of Degenerate Case IIIA.** Below, to explain Theorem 3.2, we provide an example of degenerate Case IIIA, where the pitfall nodes $P(\rho, \theta^{\pm}) = P(\bar\rho, \bar\theta^{\pm})$ of (3.12) satisfy (3.28). Choose $R = 0.4, a = 0.2$ and $R_1 = 0.19$. Eq. (3.36) is satisfied, since $R_1 = 0.19 > 0.4^2 = R^2$. We have from (3.13) and (3.29)

$$\mu = 2\frac{\ln R_1}{\ln R} - 1 = 2.62, \quad 0.4 = R \le \rho \le \frac{\ln R_1}{\ln \frac{R_1}{R}} a = 0.446. \tag{3.43}$$

Hence the pitfall notes are found for $\rho \in [0.4, 0.446]$. Then $\bar\rho$ is given as (3.12), and θ is obtained from Figure 1,

$$\cos\theta = \frac{\bar\rho^2 - \rho^2 - a^2}{2\rho a}. \tag{3.44}$$

For $\rho = R = 0.4$, we have from (3.12)

$$\bar\rho = \sqrt{\frac{\rho^2 - a^2}{\mu}} = \sqrt{\frac{0.4^2 - 0.2^2}{2.62}} = 0.2140, \tag{3.45}$$

and then from (3.44)

$$\cos\theta = \frac{(0.2140)^2 - (0.4)^2 - (0.2)^2}{2 \times 0.4 \times 0.2} = -0.9637. \tag{3.46}$$

Then we have $\theta = 164.5°$, and find the node $Q^+ = (0.4, 164.5°)$ in Figure 4, which corresponds to the left boundary point Q of curve $\widehat{QT}$ in Figure 3. Hence, when $\rho \in [0.4, 0.446]$, the pitfall nodes (ρ, θ) are located with $\theta \in [164.5°, 195.5°]$, very closely to the most left exterior boundary point at $(-R, 0)$. If the exterior boundary ∂S_R is alike a face of human being, the contour of pitfall nodes of this degenerate example just alike the edge of the left ear, see Figure 4.

When the general collocation equations (3.17) are used to replace (2.23), and when all $2M+1$ pitfall nodes (ρ_i, θ_i) are chosen, the algorithm singularity of (2.25) must occur, due to the above analysis. The numerical solutions can be obtained via

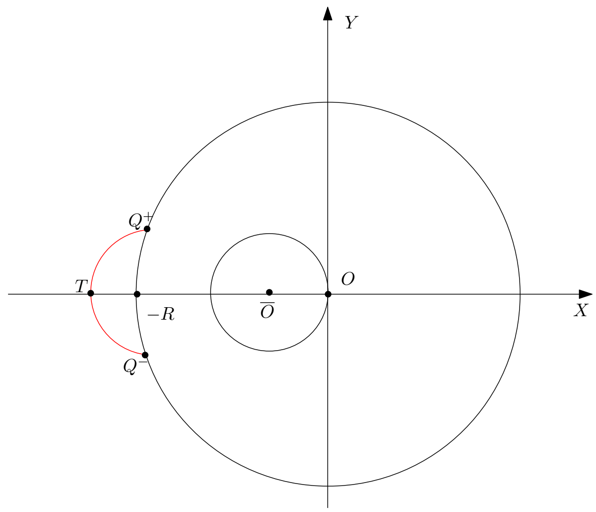

FIG. 4. An ear-edge contour of full paths of pitfall nodes for Case IIIA, where points $Q^{\pm}$ respond to point Q in Figure 3.

the truncated singular value decomposition (TSVD), where large condition numbers are obtained, see [11]. Moreover, the accuracy of numerical solutions from this Degenerate Case IIIA is poor, since the pitfall nodes are located, only nearly to point $(-R, 0)$. Therefore, we do not provide the detailed algorithms, nor carry out the computation as done in [11].

Let us compare Degenerate Case IIIA to the Degenerate Case III in [11]. The Degenerate Case III exists for all cases of $R < 1$, and their pitfall nodes are located on an exterior closed contour. In contrast, the Degenerate Case IIIA exists for $R \le R^* < 1$ under the limitation (3.28), and their pitfall nodes are located only on the left plane $x < -\frac{a}{2}$. Hence, the Degenerate Case IIIA is rarely useful in applications, because the $2M+1$ exterior nodes should be located on a closed contour, for better accuracy.

In summary, the dual techniques, type II-I, has a little risk of degenerate scales. Degenerate Case I can be avoided if $\rho = R + \epsilon$ with constant $\epsilon \ge 0$ and $M \ge 1$. Degenerate Case IIIA will not happen, if the exterior field nodes are located on a closed contour. For other cases, Degenerate Case IIIA is very rare to happen; see the example in Section 3.3. Hence, the possibility of algorithm singularity is very slight, compared with Degenerate Case III of the NFM given in [11]. This provides a strict analysis of dual techniques for unique solutions and the non-singularity of the dual algorithms, thus to remove the degenerate scales. For algorithm singularity of the dual BEM, an analysis using the SVD is reported in [5].

Remark 3.1. For the CHEEF [2, 3], type I-I is chosen, accompanied with only one more equation of (2.15) at node (ρ^*, θ^*),

$$\mathcal{D}_{ext}(\rho^*, \theta^*; \bar{\rho}^*, \bar{\theta}^*) = 0, \quad \rho^* \ge R. \tag{3.47}$$

Eq. (3.47) can be regarded as an extra-constraint of the unknown coefficients, p_k and $\bar{p}_k$. For type I-I, we may solicit the conservative law in [9],

$$Rp_0 + R_1 \bar{p}_0 = 0, \tag{3.48}$$

which is called the conservative schemes. Evidently, Eq. (3.48) is much simpler than (3.47). By using the overdetermined system (see [10]), the stability is as good as that of the dual techniques in Section 4.1, and the optimal convergence rates can be achieved by following [8, 13]. Hence, the conservative schemes are more effective than the CHEEF in application; details will appear elsewhere.

4. Analysis for Dual Techniques

For numerical algorithms, the existence and unique solutions are essential. However, the errors and stability are the core of numerical analysis and scientific computing. In this section, for the dual techniques, type II-I, not only can the best stability be obtained, but also the optimal convergence rates may be achieved.

4.1. Stability Analysis. For simplicity, we consider a simple case: (a) $M = N$, (b) the symmetric cases with $q_k = \bar{q}_k = 0$, and (c) the same system of polar coordinates (i.e.,$(\bar{\rho}, \bar{\theta}) = (\rho, \theta)$). In this case, there exist no degenerate scales, since Eq. (3.7) does not hold. We choose the IFM, and obtain from (2.15) at $\rho = R$,

$$
\begin{aligned}
\mathcal{D}_{ext}(\rho,\theta) &= \frac{1}{2R}\sum_{k=1}^{M} a_k k \cos k\theta - \frac{1}{2R}\sum_{k=1}^{M} \bar{a}_k k (\frac{R_1}{R})^k \cos k\theta \\
&-\Big\{p_0 + \frac{1}{2}\sum_{k=1}^{M} p_k \cos k\theta + (\frac{R_1}{R})\bar{p}_0 + \frac{1}{2}\sum_{k=1}^{N} \bar{p}_k (\frac{R_1}{R})^{k+1} \cos k\theta\Big\} = 0,
\end{aligned}
\tag{4.1}
$$

and from (2.11) at $\bar{\rho} = R_1$,

$$
\begin{aligned}
\mathcal{L}_{int}(\rho,\theta) &= a_0 - \bar{a}_0 - \frac{1}{2}\sum_{k=1}^{M} \bar{a}_k \cos k\bar{\theta} + \frac{1}{2}\sum_{k=1}^{M} a_k (\frac{R_1}{R})^k \cos k\theta \\
&-\Big\{R_1(\ln R_1)\bar{p}_0 - \frac{R_1}{2}\sum_{k=1}^{M}\frac{1}{k}\bar{p}_k \cos k\theta + R(\ln R)p_0 \\
&-\frac{R}{2}\sum_{k=1}^{M}\frac{1}{k}(\frac{R_1}{R})^k p_k \cos k\theta\Big\} = 0.
\end{aligned}
\tag{4.2}
$$

Eqs. (4.1) and (4.2) lead to

$$
p_0 + (\frac{R_1}{R})\bar{p}_0 + \frac{1}{2}\sum_{k=1}^{M}(p_k + \bar{p}_k(\frac{R_1}{R})^{k+1})\cos k\theta = f_1(\theta),
\tag{4.3}
$$

$$
-R(\ln R)p_0 - R_1(\ln R_1)\bar{p}_0 + \frac{1}{2}\sum_{k=1}^{M}\frac{1}{k}(p_k R(\frac{R_1}{R})^k + \bar{p}_k R_1)\cos k\theta = f_2(\theta),
\tag{4.4}
$$

where the functions $f_1(\theta)$ and $f_2(\theta)$ are independent of p_k and $\bar{p}_k$. We choose $2M + 2$ collocation equations,

$$
\frac{\sqrt{w_j}}{M}\mathcal{D}_{ext}(R, jh) = \frac{\sqrt{w_j}}{M} f(jh), \quad j = 0, 1, ..., M,
\tag{4.5}
$$

$$
\sqrt{w_j}\mathcal{L}_{int}(R_1, jh) = \sqrt{w_j}\, g(jh), \quad j = 0, 1, ..., M,
\tag{4.6}
$$

where $h = \frac{2\pi}{2M+1}$, and weights $w_0 = 1$ and $w_j = 2$ for $j \geq 1$. Eqs. (4.5) and (4.6) lead to the linear algebraic equations,

$$
\mathbf{F}\mathbf{x} = \mathbf{b},
\tag{4.7}
$$

where the matrix $\mathbf{F} \in R^{n\times n}$, the unknown vector $\mathbf{x}(\in R^n) = [p_0, p_k, q_k, \bar{p}_0, \bar{p}_k, \bar{q}_k]^T$, and $n = 2M+2$. The unknown coefficients can be obtained by solving (4.7). Denote matrix $\mathbf{B} = Diag[\mathbf{B_0}, \mathbf{B_1}, ...\mathbf{B_M}]$, where the matrices $\mathbf{B_k} \in R^{2\times 2}$ are defined as

$$\mathbf{B_0} = \begin{pmatrix} \frac{1}{M} & \frac{1}{M}\frac{R_1}{R} \\ -R(\ln R) & -R_1(\ln R_1) \end{pmatrix}, \tag{4.8}$$

$$\mathbf{B_k} = \frac{1}{2}\begin{pmatrix} \frac{1}{M} & \frac{1}{M}(\frac{R_1}{R})^{k+1} \\ \frac{R}{k}(\frac{R_1}{R})^k & \frac{R_1}{k} \end{pmatrix}, \quad k = 1, 2, ..., M. \tag{4.9}$$

Lemma 4.1. *For matrices* $\mathbf{B_k}$ *in (4.9) and (4.8), there exist the bounds,*

$$\sigma_0^+ \le C, \quad \sigma_0^- \ge c_0\frac{1}{M}, \tag{4.10}$$

$$\sigma_k^+ \le C\frac{1}{k}, \quad \sigma_k^- \ge c_0\frac{1}{M}, \quad k \ge 1, \tag{4.11}$$

where C *and* $c_0(> 0)$ *are two positive constants independent of* M*, and* $\sigma_k^{\pm}$ *are two singular values of matrices* $\mathbf{B_k}$*.*

Proof. The determinant of $\mathbf{B_0}$ in (4.8) is given by

$$Det(\mathbf{B_0}) = \frac{R_1}{M}(\ln R - \ln R_1) = \frac{R_1}{M}\ln(\frac{R}{R_1}) > 0. \tag{4.12}$$

To find two singular values $\sigma_0^{\pm}$ of matrix $\mathbf{B_0}$, we seek the eigenvalues of matrix $\mathbf{B_0^T B_0}$, denoted by

$$\mathbf{B_0^T B_0} = \begin{pmatrix} \frac{1}{M^2} + R^2(\ln R)^2 & \frac{1}{M^2}\frac{R_1}{R} + RR_1(\ln R)(\ln R_1) \\ \frac{1}{M^2}\frac{R_1}{R} + RR_1(\ln R)(\ln R_1) & \frac{1}{M^2}\{\frac{R_1}{R}\}^2 + R_1^2(\ln R_1)^2 \end{pmatrix}. \tag{4.13}$$

From (4.12), we have the determinant

$$Det(\mathbf{B_0^T B_0}) = \{Det(\mathbf{B_0})\}^2 = \frac{R_1^2}{M^2}\{\ln(\frac{R}{R_1})\}^2 > 0. \tag{4.14}$$

Since matrix $\mathbf{B_0^T B_0}$ is symmetric and positive definite, we have

$$\begin{aligned} \lambda_0^+(\mathbf{B_0^T B_0}) &\le \lambda_0^+(\mathbf{B_0^T B_0}) + \lambda_0^-(\mathbf{B_0^T B_0}) \\ &= \frac{1}{M^2} + R^2(\ln R)^2 + \frac{1}{M^2}\{\frac{R_1}{R}\}^2 + R_1^2(\ln R_1)^2 \le C, \end{aligned} \tag{4.15}$$

and then from (4.14)

$$\lambda_0^-(\mathbf{B_0^T B_0}) = \frac{Det(\mathbf{B_0^T B_0})}{\lambda_0^+(\mathbf{B_0^T B_0})} \ge c_0\frac{1}{M^2}. \tag{4.16}$$

The desired results (4.10) follow from

$$\sigma_k^{\pm} = \sigma_k^{\pm}(\mathbf{B_k}) = \sqrt{\lambda_k^{\pm}(\mathbf{B_k^T B_k})}, \quad k = 0, 1, ..., M. \tag{4.17}$$

Next, we prove (4.11). The determinant of (4.9) is given by

$$Det(\mathbf{B_k}) = \frac{R_1}{2kM}[1 - (\frac{R_1}{R})^{2k}] > 0, \quad k \ge 1. \tag{4.18}$$

The matrices $\mathbf{B_k^T B_k}(k \ge 1)$ are denoted by

$$\mathbf{B_k^T B_k} = \frac{1}{4}\begin{pmatrix} \frac{1}{M^2} + \frac{R^2}{k^2}(\frac{R_1}{R})^{2k} & \frac{1}{M^2}(\frac{R_1}{R})^{k+1} + \frac{RR_1}{k^2}(\frac{R_1}{R})^k \\ \frac{1}{M^2}(\frac{R_1}{R})^{k+1} + \frac{RR_1}{k^2}(\frac{R_1}{R})^k & \frac{R_1^2}{k^2} + \frac{R_1^2}{M^2}(\frac{R_1}{R})^{2k+2} \end{pmatrix}. \tag{4.19}$$

Similarly, we have

$$\lambda_k^+(\mathbf{B_k^T B_k}) \le \frac{1}{4}\Big\{\frac{1}{M^2} + \frac{R^2}{k^2}(\frac{R_1}{R})^{2k} + \frac{R_1^2}{k^2} + \frac{R_1^2}{M^2}(\frac{R_1}{R})^{2k+2}\Big\} \le C\frac{1}{k^2}, \quad k \ge 1,$$

and then from (4.18)

$$\lambda_k^-(\mathbf{B_k^T B_k}) = \frac{Det(\mathbf{B_k^T B_k})}{\lambda_k^+(\mathbf{B_k^T B_k})} = \frac{\{Det(\mathbf{B_k})\}^2}{\lambda_k^+(\mathbf{B_k^T B_k})} \ge c_0\frac{1}{M^2}. \tag{4.20}$$

The desired results (4.11) follow from (4.17), and this completes the proof of Lemma 4.1. □

First, we cite the following lemma from [14].

Lemma 4.2. *There exists the orthogonality of discrete Fourier series for $k, \ell \le N$,*

$$\sum_{j=0}^{M} w_j \cos(kjh)\cos(\ell jh) = \begin{cases} 2M+1, & k=\ell=0, \\ M+\frac{1}{2}, & k=\ell\ge 1, \\ 0, & k\ne \ell, \end{cases} \tag{4.21}$$

where $h = \frac{2\pi}{2M+1}$, and the weights $w_0 = 1$ and $w_j = 2$ for $j \ge 1$.

Theorem 4.1. *Let $(\bar\rho, \bar\theta) = (\rho, \theta)$ and $M = N$ be given. For the dual techniques from (4.5) and (4.6) at nodes $Q \in \partial S$, the condition number has the bound,*

$$Cond = O(M). \tag{4.22}$$

Proof. We have

$$\mathbf{x}^T\mathbf{F}^T\mathbf{F}\mathbf{x} = \sum_{j=0}^{N} w_j\Big\{\frac{1}{M^2}\mathcal{D}_{ext}^2(R, jh) + \mathcal{L}_{int}^2(R_1, jh)\Big\}, \tag{4.23}$$

where the weights $w_0 = 1$ and $w_j = 2$ for $j \ge 1$. We obtain from Lemma 4.2

$$\begin{aligned}
&\sum_{j=0}^{M} w_j \frac{1}{M^2}\mathcal{D}_{ext}^2(R, jh) \\
&= \frac{1}{M^2}\sum_{j=0}^{M} w_j\Big\{p_0 + (\frac{R_1}{R})\bar p_0 + \frac{1}{2}\sum_{k=1}^{M}(p_k + \bar p_k(\frac{R_1}{R})^{k+1})\cos kjh\Big\}^2 \\
&= \frac{1}{M^2}\sum_{j=0}^{M} w_j\Big\{p_0 + (\frac{R_1}{R})\bar p_0 + \frac{1}{2}\sum_{k=1}^{M}(p_k + \bar p_k(\frac{R_1}{R})^{k+1})\cos kjh\Big\} \\
&\times\Big\{p_0 + (\frac{R_1}{R})\bar p_0 + \frac{1}{2}\sum_{\ell=1}^{M}(p_\ell + \bar p_\ell(\frac{R_1}{R})^{\ell+1})\cos \ell jh\Big\} \\
&= (M+\frac{1}{2})\Big\{\frac{2}{M^2}(p_0 + (\frac{R_1}{R})\bar p_0)^2 + \frac{1}{4M^2}\sum_{k=1}^{M}(p_k^2 + \bar p_k^2(\frac{R_1}{R})^{k+1})^2\Big\}.
\end{aligned} \tag{4.24}$$

Similarly, we have

$$
\begin{aligned}
(4.25)\qquad &\sum_{j=0}^{M} w_j \mathcal{L}^2_{int}(R_1, jh)\\
&= \sum_{j=0}^{M} w_j \Big\{ - R(\ln R)p_0 - R_1(\ln R_1)\bar{p}_0 + \frac{1}{2}\sum_{k=1}^{M}(\frac{1}{k}(p_k R(\frac{R_1}{R})^k + \bar{p}_k R_1)\cos(kjh)\Big\}^2\\
&= (M+\frac{1}{2})\Big\{2(R(\ln R)p_0 + R_1(\ln R_1)\bar{p}_0)^2 + \frac{1}{4}\sum_{k=1}^{M}\frac{1}{k^2}(p_k R(\frac{R_1}{R})^k + \bar{p}_k R_1)^2\Big\}.
\end{aligned}
$$

Combining (4.23)-(4.25) yields

$$
\begin{aligned}
(4.26)\quad \mathbf{x}^T\mathbf{F}^T\mathbf{F}\mathbf{x} &= (M+\frac{1}{2})\Big\{\frac{2}{M^2}(p_0 + (\frac{R_1}{R})\bar{p}_0)^2 + 2(R(\ln R)p_0 + R_1(\ln R_1)\bar{p}_0)^2\\
&+\frac{1}{4}\sum_{k=1}^{M}\{(\frac{1}{M^2}(p_k^2 + \bar{p}_k^2(\frac{R_1}{R})^{k+1})^2 + \frac{1}{k^2}(p_k R(\frac{R_1}{R})^k + \bar{p}_k R_1)^2\}\Big\}\\
&= (2M+1)\mathbf{x}_0^T\mathbf{B}_0^T\mathbf{B}_0\mathbf{x}_0 + (M+\frac{1}{2})\sum_{k=1}^{N}\mathbf{x}_k^T\mathbf{B}_k^T\mathbf{B}_k\mathbf{x}_k,
\end{aligned}
$$

where vectors $\mathbf{x_k} = (p_k, \bar{p}_k)^T$, and matrices $\mathbf{B_k}$ are defined in (4.8) and (4.9). Since

$$
(4.27)\qquad \sigma_{\max}(\mathbf{F}) = \sqrt{\max_{\mathbf{x}\neq 0}\frac{\mathbf{x}^T\mathbf{F}^T\mathbf{F}\mathbf{x}}{\mathbf{x}^T\mathbf{x}}},\quad \sigma_{\min}(\mathbf{F}) = \sqrt{\min_{\mathbf{x}\neq 0}\frac{\mathbf{x}^T\mathbf{F}^T\mathbf{F}\mathbf{x}}{\mathbf{x}^T\mathbf{x}}},
$$

where vector $\mathbf{x} = [\mathbf{x_0}, \mathbf{x_1}, ...\mathbf{x_M}]^T$. We have from (4.26), (4.27) and Lemma 4.1,

$$
(4.28)\qquad \sigma_{\max}(\mathbf{F}) = \sqrt{\lambda_{\max}(\mathbf{F}^T\mathbf{F})} \leq C\sqrt{M}\sigma_{\max}(\mathbf{B}) \leq C\sqrt{M},
$$

$$
(4.29)\qquad \sigma_{\min}(\mathbf{F}) = \sqrt{\lambda_{\min}(\mathbf{F}^T\mathbf{F})} \geq c_0\sqrt{M}\sigma_{\min}(\mathbf{B}) \geq \frac{c_0}{\sqrt{M}},
$$

where $c_0(>0)$ and C are two constants independent of M. The desired result (4.22) follows from (4.28) and (4.29). This completes the proof of Theorem 4.1. □

4.2. **Brief Error Analysis.** The NFM at nodes $Q \in \partial S$ is equivalent to the interior filed method (IFM), which can be classified as the Trefftz method (TM), see [8, 10]. We may derive the error bounds by following the outlines of analysis in [13, 16]. In the dual techniques, the first kind NFM (2.11) at $Q \in \partial S_{R_1}$ is used, which is equivalent to the solution (2.13) satisfying the Dirichlet condition $u = f$ on ∂S_{R_1}, while the second kind NFM (2.15) at $Q \in \partial S_R$ is used, which is equivalent to the solution (2.13) satisfying the Neumann condition $u_\nu = g$ on ∂S_R. The dual techniques may be regarded as the Trefftz method for the mixed boundary value problems (simply called the mixed problems) of both Dirichlet and Neumann conditions in [12, 15, 16]. Define the energy

$$
(4.30)\qquad I(v) = \omega^2\int_{\partial S_R}(v_\nu - g(v))^2 ds + \int_{\partial S_{R_1}}(v-f)^2 ds,
$$

where $v = u_{M-N}$ is given in (2.13), and f is the known function (2.5) with the given coefficients $\bar{a}_k$ and $\bar{b}_k$. However, the function $g(v)$ in (2.4) is not given explicitly, since p_k and q_k are unknown and to be sought. For the Dirichlet condition (2.3) absenting in (4.30), the coefficients a_k and b_k are still given in advance. Then, for

(2.15) and (2.11), only coefficients, $p_k, q_k, \bar{p}_k$ and $\bar{q}_k$, are unknowns, and the total number of unknowns is still $2(M+N+1)$. The weight $\omega = \frac{1}{M}$ in (4.30) is optimal in convergence for the mixed problems of Dirichlet and the Neumann conditions, see [12, 15, 16]. Denote the set of (2.13) as V_{M-N} with the unknown coefficients $p_k, q_k, \bar{p}_k$ and $\bar{q}_k$. Based on the equivalence of (2.15) and (2.11) to the the solution (2.13) of the mixed problem, the dual techniques may read: To seek u_{M-N} such that

$$I(u_{M-N}) = \min_{v \in V_{M-N}} I(v). \tag{4.31}$$

When there exist the numerical integrations, Eq. (4.31) leads to

$$\hat{I}(u_{M-N}) = \min_{v \in V_{M-N}} \hat{I}(v), \tag{4.32}$$

where

$$\hat{I}(v) = \omega^2 \widehat{\int}_{\partial S_R} (v_\nu - g(v))^2 ds + \widehat{\int}_{\partial S_{R_1}} (v - f)^2 ds, \tag{4.33}$$

where $\widehat{\int}_{\partial S_R}$ and $\widehat{\int}_{\partial S_{R_1}}$ are the approximations by the trapezoidal (or Gaussian) rule.

Let us estimate the errors of the dual techniques. First, assume that the solution is smooth such that

$$(u \in H^p(\partial S_R)) \wedge (u_\nu \in H^p(\partial S_R)), \quad p \geq 2, \tag{4.34}$$

$$(u \in H^q(\partial S_{R_1})) \wedge (u_{\bar{\nu}} \in H^{q-1}(\partial S_{R_1})), \quad q \geq 2. \tag{4.35}$$

Second, we assume that the Fourier expansion coefficients $a_k, b_k, \bar{a}_k$ and $\bar{b}_k$ in (2.3) and (2.5) are given exactly,

$$a_0 = \frac{1}{2\pi}\int_0^{2\pi} u(R,\theta)d\theta, \quad \bar{a}_0 = \frac{1}{2\pi}\int_0^{2\pi} u(R_1,\bar{\theta})d\bar{\theta}, \tag{4.36}$$

$$a_k = \frac{1}{\pi}\int_0^{2\pi} u(R,\theta)\cos k\theta d\theta, \;\; b_k = \frac{1}{\pi}\int_0^{2\pi} u(R,\theta)\sin k\theta d\theta, \tag{4.37}$$

$$\bar{a}_k = \frac{1}{\pi}\int_0^{2\pi} u(R_1,\bar{\theta})\cos k\bar{\theta} d\bar{\theta}, \;\; \bar{b}_k = \frac{1}{\pi}\int_0^{2\pi} u(R_1,\bar{\theta})\sin k\bar{\theta} d\bar{\theta}. \tag{4.38}$$

For the exterior boundary condition (2.4), denote the unknown function $g(v)$ and the solution derivatives,

$$g(v) = \tilde{u}_\nu(v) = \hat{D}u_M(\partial S_R) = p_0 + \sum_{k=1}^{M}\{p_k \cos k\theta + q_k \sin k\theta\}, \quad on \quad \partial S_R, \tag{4.39}$$

$$u_\nu = \hat{D}u_\infty(\partial S_R) = p_0 + \sum_{k=1}^{\infty}\{p_k \cos k\theta + q_k \sin k\theta\}, \quad on \quad \partial S_R. \tag{4.40}$$

Their errors are given by

$$\begin{aligned} \hat{D}R_M = u_\nu - g(v) &= \hat{D}u_\infty(\partial S_R) - \hat{D}u_M(\partial S_R) \\ &= \sum_{k=M+1}^{\infty}\{p_k \cos k\theta + q_k \sin k\theta\}. \end{aligned} \tag{4.41}$$

We obtain the bounds from [13]

$$\|\hat{D}R_M\|_{0,\partial S_R} = \|(\hat{D}u_\infty - \hat{D}u_M)\|_{0,\partial S_R} \le C\frac{1}{M^{p-1}}\|u_\nu\|_{p-1,\partial S_R}. \tag{4.42}$$

Define the norm

$$\|u-v\|_0^* = \sqrt{I(v)}, \tag{4.43}$$

where $I(v)$ is given in (4.30). Since $f = u$ on ∂S_{R_1} and $u_\nu = \hat{D}u_\infty(\partial S_R)$, we have from (4.41),

$$\begin{aligned} \{\|u-v\|_0^*\}^2 &\\ &= \omega^2\int_{\partial S_R}(v_\nu - u_\nu + \hat{D}u_\infty(\partial S_R) - g(v))^2 ds + \int_{\partial S_{R_1}}(u-v)^2 ds \\ &= \omega^2\int_{\partial S_R}(u_\nu - v_\nu - \hat{D}R_M)^2 ds + \int_{\partial S_{R_1}}(u-v)^2 ds. \end{aligned} \tag{4.44}$$

From (4.31), there exists the bound,

$$\|u-u_{M-N}\|_0^* \le \inf_{v\in V_{M-N}}\{\omega\|u_\nu - v_\nu - \hat{D}R_M\|_{0,\partial S_R} + \|u-v\|_{0,\partial S_{R_1}}\}. \tag{4.45}$$

Let $\omega = \frac{1}{M}$ and $v = u^*_{M-N}$, where u^*_{M-N} is the solution with true Fourier expansion coefficients. Then we obtain the optimal convergence rates,

$$\begin{aligned} \|u-u_{M-N}\|_0^* &\le \omega\|u_\nu - (u^*_{M-N})_\nu - \hat{D}R_M\|_{0,\partial S_R} + \|u-(u^*_{M-N})\|_{0,\partial S_{R_1}} \\ &= \frac{1}{M}(\|(R_{M-N}u)_\nu\|_{0,\partial S_R} + \|\hat{D}R_M\|_{0,\partial S_R}) + \|R_{M-N}u\|_{0,\partial S_{R_1}}, \end{aligned} \tag{4.46}$$

where $(R_{M-N}u)_\nu$ is the remainder of derivatives $(u^*_{M-N})_\nu$. Based on (4.46), (4.42) and [16, 13, 21], we may obtain the following theorem.

Theorem 4.2. *Suppose that the smooth solution satisfy (4.34) and (4.35), and that the exact Fourier expansion coefficients $a_k, b_k, \bar{a}_k$ and $\bar{b}_k$ as in (4.36)-(4.38) are given. Then there exist the error bounds of the solutions from the dual techniques, (2.15) at $\rho = R$ and (2.11) at $\bar{\rho} = R_1$,*

$$\begin{aligned} \|u-u_{M-N}\|_0^* \le C\{&\frac{1}{M^p}(\|u\|_{p,\partial S_R} + \|u_\nu\|_{p-1,\partial S_R}) \\ &+\frac{1}{N^q}(\|u\|_{q,\partial S_{R_1}} + \|u_{\bar{\nu}}\|_{q-1,\partial S_{R_1}})\}, \end{aligned} \tag{4.47}$$

where C is a constant independent of M and N.

5. Numerical Experiments

5.1. **For Model Problem.** Choose the simple Dirichlet boundaries of (2.3) and (2.5)

$$u = a_0 = 1 \text{ on } \partial S_R, \quad u = \bar{a}_0 = 0 \text{ on } \partial S_{R_1}. \tag{5.1}$$

Model Problem of Dirichlet problems of Laplace's equation is defined by (5.1) with $R = 2.5$ and $R_1 = 1$. The true solution of Model Problem is found in [14, 19]

$$u^{Model}(\rho,\theta) = u^{Model}(\bar{\rho},\bar{\theta}) = \frac{1}{2\ln 2}\ln\{\frac{16\bar{\rho}^2 + 1 + 8\bar{\rho}\cos\bar{\theta}}{\bar{\rho}^2 + 16 + 8\bar{\rho}\cos\bar{\theta}}\}, \tag{5.2}$$

where $(\bar{\rho},\bar{\theta})$ are the polar coordinates of S_{R_1} with the origin $(-1,0)$, and (ρ,θ) are obtained from the transformation (2.1). The normal derivatives can be obtained from (5.2) in [14]. We carry out the computation by the dual techniques. By using symmetry, the interior solutions are given from (2.13),

$$u_{M-N} = u_{M-N}(\rho,\theta;\bar\rho,\bar\theta) = a_0 - R(\ln R)p_0 - R_1(\ln\bar\rho)\bar p_0 + \frac{R}{2}\sum_{k=1}^{M}\frac{1}{k}(\frac{\rho}{R})^k p_k\cos k\theta + \frac{R_1}{2}\sum_{k=1}^{N}\frac{1}{k}(\frac{R_1}{\bar\rho})^k\bar p_k\cos k\bar\theta, \quad (r,\theta)\in S. \tag{5.3}$$

Also two explicit equations are given from (2.15) and (2.11),

$$\mathcal{D}_{ext}(\rho,\theta;\bar\rho,\bar\theta) = \frac{\partial}{\partial\rho}\mathcal{L}_{ext}(\rho,\theta;\bar\rho,\bar\theta) = -\Big\{(\frac{R}{\rho})p_0 + (\frac{R_1}{\bar\rho})\bar p_0\cos(\theta-\bar\theta) + \frac12\sum_{k=1}^{M}(\frac{R}{\rho})^{k+1}p_k\cos k\theta + \frac12\sum_{k=1}^{N}(\frac{R_1}{\bar\rho})^{k+1}\bar p_k\cos((k+1)\bar\theta-\theta)\Big\} = 0, \quad \rho\ge R, \tag{5.4}$$

and

$$\mathcal{L}_{int}(\rho,\theta;\bar\rho,\bar\theta) = -\bar a_0 + a_0 - \Big\{R_1(\ln R_1)\bar p_0 + R(\ln R)p_0 - \frac{R_1}{2}\sum_{k=1}^{N}\frac{1}{k}(\frac{\bar\rho}{R_1})^k\bar p_k\cos k\bar\theta - \frac{R}{2}\sum_{k=1}^{M}\frac{1}{k}(\frac{\rho}{R})^k p_k\cos k\theta\Big\} = 0, \quad \bar\rho\le R_1. \tag{5.5}$$

The number of unknown coefficients is $M+N+2$. In computation, we choose the nodes $Q\in\partial S_R\cup\partial S_{R_1}$, and obtain the following $M+M+2$ collocation equations,

$$\sqrt{w_j}\frac{1}{M}\mathcal{D}_{ext}(R,j\Delta\theta;\bar\rho_j,\bar\theta_j) = 0, \quad j=0,1,...,M, \tag{5.6}$$

$$\sqrt{w_j}\mathcal{L}_{int}(\rho_j,\theta_j;R_1,j\Delta\bar\theta) = 0, \quad j=0,1,...,N, \tag{5.7}$$

where $\Delta\theta=\frac{2\pi}{2M+1}$, $\Delta\bar\theta=\frac{2\pi}{2N+1}$, and $w_0=1$ and $w_j=2(j\ge1)$ from the stability analysis in Section 4.1. Eqs. (5.6) and (5.7) lead to the linear algebraic equations,

$$\mathbf{A}\mathbf{x}=\mathbf{b}, \tag{5.8}$$

where the matrices $\mathbf{A}\in R^{n\times n}$, the vector $\mathbf{x}(\in R^n)=\{p_k,\bar p_k\}^T$ and $n=M+N+2$. The Gaussian elimination is used to seek the coefficients p_k and $\bar p_k$, and the solution is given by (5.3). Note that for the same Model problem of Dirichlet problem of Laplace's equation, Eq. (5.6) is different from that in [14]. The derivatives (5.4) are of the second kind NFM. The second kind NFM is usually applied to the Neumann problems in [10], where coefficients a_k and $\bar a_k$ are unknown. In contrast, coefficients p_k and $\bar p_k$ in (5.3) are unknown.

Define the norm of errors as

$$\|\varepsilon\|_H = \{\frac{1}{M^2}\|\varepsilon_\nu\|^2_{0,S_R} + \|\varepsilon\|^2_{0,S_{R_1}}\}^{\frac12}, \quad \|\varepsilon\|_h = \{\|\varepsilon\|^2_{0,S_R} + \|\varepsilon\|^2_{0,S_{R_1}}\}^{\frac12}, \tag{5.9}$$

where $\varepsilon=u-u_{M-N}$. The condition number and the effective condition number are defined in [17] by

$$\text{Cond} = \frac{\sigma_{\max}}{\sigma_{\min}}, \quad \text{Cond\_eff} = \frac{\|\mathbf{b}\|}{\sigma_{\min}\|\mathbf{x}\|}, \tag{5.10}$$

where $\|\mathbf{x}\|$ is the 2- norm of vector $\mathbf{x}$, and $\sigma_{\max}$ and $\sigma_{\min}$ are the maximal and the minimal singular values of matrix $\mathbf{A}$, respectively. The effective condition number Cond_eff is smaller and even much smaller than the Cond for numerical partial differential equations (PDE). The Cond_eff is a better criterion for numerical stability than the Cond, and a systematic analysis is reported in Li et al. [17].

For Model Problem, different N are chosen for $M = 20$, and errors and condition numbers are listed in Table1.

N	$\|\varepsilon\|_{0,S_R}$	$\|\varepsilon\|_{0,S_{R_1}}$	$\|\varepsilon_\nu\|_{0,S_R}$	$\|\varepsilon_\nu\|_{0,S_{R_1}}$	Cond	Cond_eff
2	8.23E-08	7.19E-02	8.49E-02	2.13E-01	26.36	3.67
4	2.89E-07	2.84E-03	2.23E-03	1.32E-02	40.68	6.78
6	4.69E-07	1.28E-04	6.12E-05	8.39E-04	55.06	10.01
8	5.36E-07	6.24E-06	4.98E-06	5.33E-05	69.25	13.23
10	5.48E-07	3.17E-07	4.50E-06	3.39E-06	83.33	16.45
12	5.49E-07	1.58E-08	4.48E-06	2.40E-07	97.35	19.67
14	5.49E-07	6.42E-10	4.48E-06	7.67E-08	111.32	22.88
16	5.49E-07	1.50E-11	4.48E-06	7.49E-08	125.28	26.09
18	5.49E-07	1.11E-13	4.48E-06	7.48E-08	139.21	29.29
20	5.49E-07	2.78E-14	4.48E-06	7.48E-08	153.14	32.50

TABLE 1. Errors and condition numbers for Model Problem by the dual techniques with $M = 20$.

From Table 1, we can see that $N = 10$ is a good choice, since the boundary error decreases insignificantly for $N \geq 10$. Hence, a better match between M and N is found as $(M,N) = (2,1)$, which is reasonable since the ratio of radius between the large circle and small circle is $(R, R_1) = (2.5, 1)$. By using $(M : N) = (2 : 1)$, the errors and condition numbers are listed in Table 2, and the coefficients in Table 3.

M	N	$\|\varepsilon\|_{0,S_R}$	$\|\varepsilon\|_{0,S_{R_1}}$	$\|\varepsilon\|_h$	$\|\varepsilon_\nu\|_{0,S_R}$	$\|\varepsilon_\nu\|_{0,S_{R_1}}$	$\|\varepsilon\|_H$	Cond	Cond_eff
4	2	1.62E-01	4.37E-02	1.68E-01	3.61E-01	3.54E-01	1.00E-01	20.54	4.13
12	6	2.29E-04	1.21E-04	2.59E-04	1.17E-03	8.92E-04	1.56E-04	50.65	10.01
20	10	5.48E-07	3.17E-07	6.33E-07	4.50E-06	3.39E-06	3.89E-07	83.33	16.45
28	14	1.54E-09	9.16E-10	1.79E-09	1.75E-08	1.33E-08	1.11E-09	115.91	22.88
36	18	4.69E-12	2.83E-12	5.48E-12	6.84E-11	5.24E-11	3.41E-12	148.43	29.29
44	22	3.70E-14	1.73E-14	4.09E-14	2.69E-13	2.23E-13	1.83E-14	180.93	35.70

TABLE 2. Errors and condition numbers for Model Problem by the dual techniques with $(M : N) = (2 : 1)$.

From Table 2, we may find the following asymptotes,

$$(5.11)\quad \|\varepsilon\|_{0,\partial S_R} = O(0.503^M),\quad \|\varepsilon\|_{0,\partial S_{R_1}} = O(0.498^M),\quad \|\varepsilon\|_h = O(0.502^M),$$

$$(5.12)\quad \|\varepsilon_\nu\|_{0,\partial S_R} = O(0.550^M),\quad \|\varepsilon_\nu\|_{0,\partial S_{R_1}} = O(0.553^M),\quad \|\varepsilon\|_H = O(0.545^M),$$

$$(5.13)\quad \mathrm{Cond}(\mathbf{A}) = O(M),\quad \mathrm{Cond\_eff}(\mathbf{A}) = O(M).$$

The condition numbers $O(M)$ in (5.13) coincide perfectly with Theorem 4.1, and the known bound Cond_eff $\leq$ Cond from [17]. The exponential convergence in (5.11) and (5.12) is consistent with the error analysis in Section 4.2, since the solution (5.2) of the model problem is highly smooth. Moreover, the coefficients in Table 3 agree with those in [14, Table 3].

5.2. **For Degenerate Case I.** Degenerate Case I is defined by (5.1) with $R = 1$ and $R_1 = 0.4$ in [11]. The true solution of Degenerate Case I can be obtained from (5.2) via a scale transformation,

$$(5.14)\quad u^{DegCase}(\rho,\theta) = u^{DegCase}(\bar\rho,\bar\theta) = \frac{1}{2\ln 2}\ln\{\frac{16(\frac{\bar\rho}{0.4})^2 + 1 + 8(\frac{\bar\rho}{0.4})\cos\bar\theta}{(\frac{\bar\rho}{0.4})^2 + 16 + 8(\frac{\bar\rho}{0.4})\cos\bar\theta}\}$$

$$= \frac{1}{2\ln 2}\ln\{\frac{100\bar\rho^2 + 1 + 20\bar\rho\cos\bar\theta}{6.25\bar\rho^2 + 16 + 20\bar\rho\cos\bar\theta}\},$$

k	p_k	k	p_k
0	**5.77078016355585**E-01	/	/
1	**-5.7707801635558**3E-01	23	**-1.37586120**243466E-07
2	**2.88539008177792**E-01	24	**6.87930607**609056E-08
3	**-1.4426950408889**4E-01	25	**-3.43965**295477178E-08
4	**7.213475204444**78E-02	26	**1.7198265**5942852E-08
5	**-3.6067376022224**1E-02	27	**-8.599132**29814495E-09
6	**1.803368801111**33E-02	28	**4.299566**88554378E-09
7	**-9.01684400555**583E-03	29	**-2.14978**273379107E-09
8	**4.508422002778**47E-03	30	**1.074891**98006346E-09
9	**-2.25421100138**814E-03	31	**-5.37445**469411618E-10
10	**1.127105500694**00E-03	32	**2.6872**3563599604E-10
11	**-5.6355275034**6028E-04	33	**-1.34361**123372839E-10
12	**2.81776375173**099E-04	34	**6.718**12040006617E-11
13	**-1.4088818758**5722E-04	35	**-3.35**897953096800E-11
14	**7.0444093793**0987E-05	36	**1.67951**970273208E-11
15	**-3.5222046896**0927E-05	37	**-8.39**693427485934E-12
16	**1.7611023448**4511E-05	38	**4.198**51901261732E-12
17	**-8.80551172**376346E-06	39	**-2.09**773153859011E-12
18	**4.402755862**15541E-06	40	**1.04**777161262283E-12
19	**-2.20137793**053615E-06	41	**-5.2**0003217803839E-13
20	**1.100688965**82678E-06	42	**2**.54517235615278E-13
21	**-5.50344482**320820E-07	43	**-1**.14031784777390E-13
22	**2.75172241**847966E-07	44	3.30950302757752E-14

k	$\bar{p}_k$	k	$\bar{p}_k$
0	**-1.44269504088896**E+00	/	/
1	**7.2134752044448**0E-01	12	**-1.719826**48393315E-07
2	**-1.803368801111**19E-01	13	**4.29956**594728619E-08
3	**4.5084220027780**8E-02	14	**-1.07489**211644045E-08
4	**-1.1271055006945**2E-02	15	**2.6872**3203976677E-09
5	**2.81776375173**729E-03	16	**-6.7180**5379975541E-10
6	**-7.0444093793**0649E-04	17	**1.6796**1000712086E-10
7	**1.7611023448**6329E-04	18	**-4.198**65452084764E-11
8	**-4.402755862**17425E-05	19	**1.0497**8988826540E-11
9	**1.100688965**37037E-05	20	**-2.62**342366797244E-12
10	**-2.7517224138**9339E-06	21	**6**.44444241894304E-13
11	**6.87930607**284316E-07	22	**-1**.20762991620560E-13

TABLE 3. The coefficients p_k and $\bar{p}_k$ at $(M : N) = (44 : 22)$ in Table 2, where "**bold**" digits highlight the same as those in [14, Table 3].

where $(\bar{\rho}, \bar{\theta})$ are the polar coordinates of S_{R_1} with the origin $(-0.4, 0)$, and (ρ, θ) are obtained from the transformation (2.1), and given by

$$\rho = \sqrt{(\bar{\rho}\cos\bar{\theta} - 0.4)^2 + (\bar{\rho}\sin\bar{\theta})^2}, \quad \cos\theta = \frac{\bar{\rho}\sin\bar{\theta}}{\rho}. \tag{5.15}$$

For Degenerate Case I, errors and condition numbers are listed in Table 4.

M	N	$\Vert\epsilon\Vert_{0,S_R}$	$\Vert\epsilon\Vert_{0,S_{R_1}}$	$\Vert\varepsilon\Vert_h$	$\Vert\epsilon_\nu\Vert_{0,S_R}$	$\Vert\epsilon_\nu\Vert_{0,S_{R_1}}$	$\Vert\varepsilon\Vert_H$	Cond	Cond_eff
4	2	1.60E-01	4.37E-02	1.66E-01	9.16E-01	9.11E-01	2.33E-01	24.73	3.64
12	6	2.29E-04	1.21E-04	2.59E-04	2.93E-03	2.23E-03	2.73E-04	70.22	10.01
20	10	5.48E-07	3.17E-07	6.33E-07	1.12E-05	8.48E-06	6.45E-07	115.82	16.45
28	14	1.54E-09	9.16E-10	1.79E-09	4.38E-08	3.33E-08	1.81E-09	161.27	22.88
36	18	4.69E-12	2.83E-12	5.48E-12	1.71E-10	1.31E-10	5.53E-12	206.65	29.29
44	22	2.93E-14	3.52E-14	4.58E-14	6.80E-13	5.68E-13	3.85E-14	252.00	35.70

TABLE 4. Errors and condition numbers For Degenerate Model I by the dual techniques with $M = 2N$, where $\varepsilon = u - u_{M-N}$.

From Table 4, we may find the following asymptotes,

(5.16) $\|\varepsilon\|_{0,\partial S_R} = O(0.497^M), \quad \|\varepsilon\|_{0,\partial S_{R_1}} = O(0.513^M), \quad \|\varepsilon\|_h = O(0.504^M),$

(5.17) $\|\varepsilon_\nu\|_{0,\partial S_R} = O(0.500^M), \quad \|\varepsilon_\nu\|_{0,\partial S_{R_1}} = O(0.502^M), \quad \|\varepsilon\|_H = O(0.500^M),$

(5.18) $\text{Cond}(\mathbf{A}) = O(M), \quad \text{Cond\_eff}(\mathbf{A}) = O(M).$

We can see that the numerical performance for Degenerate Case I is as good as that for Model Problem in Section 5.1, to verify the analysis of dual techniques in this paper. The coefficients are also listed in Table 5; they also agree with those in [11, Table 3] by the NFM with $\epsilon = \bar{\epsilon} = 0$ via the truncated singular value decomposition (TSVD). We only list the leading coefficients from Table 5,

$$p_1 = \mathbf{-1.44269504088896}, \tag{5.19}$$
$$\bar{p}_0 = \mathbf{-3.60673760222224}2, \quad \bar{p}_1 = \mathbf{1.80336880111112}0,$$

where "**bold**" digits highlight the same as those in [11, Table]. For Degenerate Case I in [11, Table 3], the TSVD is more complicated than the Gaussian elimination used in the dual techniques. This is an advantage of dual techniques, which have been widely used in engineering computation (see [4, 20]).

k	p_k	k	p_k
0	1.44269504088895E+00	/	/
1	-1.44269504088896E+00	23	-3.43965304247170E-07
2	7.21347520444478E-01	24	1.71982652283100E-07
3	-3.60673760222249E-01	25	-8.59913267445459E-08
4	1.80336880111115E-01	26	4.29956634897546E-08
5	-9.01684400555537E-02	27	-2.14978317721785E-08
6	4.50842200277822E-02	28	1.07489153440605E-08
7	-2.25421100138959E-02	29	-5.37445824887292E-09
8	1.12710550069496E-02	30	2.68722897199011E-09
9	-5.63552750347122E-03	31	-1.34361463719127E-09
10	2.81776375173187E-03	32	6.71807235285920E-10
11	-1.40888187586139E-03	33	-3.35904084406186E-10
12	7.04440937929368E-04	34	1.67951265507791E-10
13	-3.52220468964682E-04	35	-8.39760091473842E-11
14	1.76110234485279E-04	36	4.19871039179853E-11
15	-8.80551172455331E-05	37	-2.09937852904675E-11
16	4.40275586266996E-05	38	1.04955242032292E-11
17	-2.20137793174572E-05	39	-5.24648315503994E-12
18	1.10068896618736E-05	40	2.61914324090401E-12
19	-5.50344483388396E-06	41	-1.30232700286596E-12
20	2.75172241898938E-06	42	6.34882450342706E-13
21	-1.37586121131514E-06	43	-2.87495539804123E-13
22	6.87930606670598E-07	44	8.17477928136056E-14

k	$\bar{p}_k$	k	$\bar{p}_k$
0	-3.60673760222242E+00	/	/
1	1.80336880111120E+00	12	-4.29956632247978E-07
2	-4.50842200277797E-01	13	1.07489166060012E-07
3	1.12710550069449E-01	14	-2.68722920754338E-08
4	-2.81776375173650E-02	15	6.71807072740393E-09
5	7.04440937933192E-03	16	-1.67951497170469E-09
6	-1.76110234483112E-03	17	4.19888322895912E-10
7	4.40275586213233E-04	18	-1.04984733471751E-10
8	-1.10068896557114E-04	19	2.62054465583958E-11
9	2.75172241307462E-05	20	-6.51422362232812E-12
10	-6.87930602418822E-06	21	1.63203912190157E-12
11	1.71982651817981E-06	22	-3.09432167389101E-13

TABLE 5. The coefficients of $(M, N) = (44, 22)$ in Table 4.

6. Concluding Remarks

Let us give a few remarks, to address the novelties of this paper.

1. Although the dual techniques have been widely used in engineering computation, to deal with algorithm singularity (see [4, 20]), there exists no strict analysis. For Laplace's equation in circular domains with circular holes, the second and the first kind NFM are used for the exterior and the interior boundaries, respectively, called the dual techniques in this paper, to remove the degenerate scales. This paper is devoted to explore a theoretical analysis to fill up some gap between theory and computation [4, 20].

2. In [11], for type I-I of the first kind NFM, two kinds of degenerate scales are found, (1) Degenerate Case I with $\rho = R = 1$, and (2) Degenerate Case III for $R_1 < R < 1$, where the field nodes may be located on a closed contour outside of ∂S_R. From Theorem 3.1, when $M \geq 1$ and the $(2M+1)$ field nodes are located on the same circle outside of S, the popular degenerate Case I of [11] can be always bypassed. The dual techniques of this paper is significant in real applications, because Degenerate Case I no longer exists.

3. There does exist Degenerate Scale IIIA of dual techniques. From Lemma 3.2, a limitation $R \leq R^* < 1$ is given in (3.28). The pitfall nodes are located only on the left plane $x < -\frac{a}{2}$. Since stability and accuracy are the important criteria for applications, Degenerate Scale IIIA is rarely useful in applications. However, the theoretical analysis of all pitfall nodes is essential for the dual techniques.

4. The stability analysis of dual techniques is explored in Theorem 4.1, to reach excellent stability. The error bounds are also provided in Theorem 4.2, to also achieve the optimal convergence rates. The theoretical analysis has been supported by the numerical experiments in Section 5.

5. For dual techniques, the solution methods are simple, since the simple Gaussian elimination, or the iteration methods, can be employed. A sequential paper of the DNFM is developed for elliptic domains with one elliptic hole, where more discovers are reported. Moreover, the dual NFM can be applied to multiple holes, circular, elliptic and arbitrary with smooth boundary. For polygonal holes and the interior holes with corners, the dual NFM is still valid to guarantee the unique solutions, provided that the suitable singular solutions near corners are introduced into the algorithms, see [18, Section 5.4]. More exploration appears elsewhere. For eigenvalue problems by the first kind NFM, the superfluous eigenvalues are infinite, and more severe difficulties are encountered in numerical computation [2]. Hence, the dual techniques may be more significant and important for eigenvalue problems. More papers and references can be found from Taiwan NTOU/MSV group.

References

[1] C.A. Brebbia, J.C.F. Telles, L.C. Wrobel, *Boundary element techniques. Theory and applications in engineering*, Springer-Verlag, Berlin etc., 1984. Zbl 0556.73086

[2] I.L. Chen, J.-T. Chen, S.-R. Kuo, M.T. Liang, *A new method for true and spurious eigensolutions of arbitrary captives using the combined Helmholtz exterior integral equation formulation method*, J. Acoust. Soc., Am, **109**:3 (2001), 982–999.

[3] J.-T. Chen, H. Han, S.-R. Kuo, S.-K. Kao, *Regularization methods for iII-conditioned system of the integral equation of the first kind with the logarithmic kernel*, Inverse Probl. Sci. Eng., **22**:7 (2014), 1176–1195. Zbl 1321.65194

[4] J.-T. Chen, H.K. Hong, *Review of dual boundary element methods with emphasis on hypersingular integrals and divergent series*, Appl. Mech. Rev.,**52**:1 (1999), 17–33.

[5] J.-T. Chen, W.S. Huang, Y. Fan, S.-K. Kao, *Revisit of the daul BEM using SVD updating technique*, J. Mechanics, **31**:5 (2015), 505–514.
[6] J.-T. Chen, W.-C. Shen, *Null-field approach for Laplace problems with circular boundaries using degenerate kernels*, Numer. Meth. PDE., **25**:1 (2009), 63–86. Zbl 1156.65097
[7] I.S. Gradshteyn, I.M. Ryzhik, *Table of Integrals, series, and products*, Academic Press, New York etc., 1980. Zbl 0521.33001
[8] H.-T. Huang, M.-G. Lee, Z.-C. Li, J.Y. Chiang, *Null field and interior field methods for Laplace's equation in actually punctured disks*, Abstr. Appl. Anal., Article ID **927873**, 2013. Zbl 07095501
[9] M.-G. Lee, Z.-C. Li, H.-T. Huang, J.Y. Chiang, *Conservative schemes and degenerate scale problems of null-field methods for Dirichlet problems of Laplace's equation*, Eng. Anal. Bound. Elem., **37**:1 (2013), 95–106. Zbl 1351.74168
[10] M.-G. Lee, Z.-C. Li, H.-T. Huang, J.Y. Chiang, *Neumann problems of Laplace's equation in circular domains with circular holes by methods of field equations*, Eng. Anal. Bound. Elem., **51** (2015), 156–173. Zbl 1403.65168
[11] M.-G. Lee, Z.-C. Li, L.P. Zhang, H.-T. Huang, J.Y. Chiang, *Algorithm singularity of the null-field method for Dirichlet problems of Laplace's equation in annular and circular domains*, Eng. Anal. Bound. Elem., **41** (2014), 160–172. Zbl 1297.74147
[12] Z.-C. Li, *Combined methods for elliptic equations with singularities, interfaces and infinities*, Mathematics and its Applications, **444**, Kluwer Academic Publishers, Dordrecht, 1998. Zbl 0909.65079
[13] Z.-C. Li, J.Y. Chiang, H.-T. Huang, M.-G. Lee, *The interior field method for Laplace's equation in circular domains with circular holes*, Eng. Anal. Bound. Elem., **67** (2016), 173–185. Zbl 1403.74308
[14] Z.-C. Li, H.-T. Huang, C.-P. Liaw, M.-G. Lee, *The null-field method of Dirichlet problems of Laplace's equation on circular domains with circular holes*, Eng. Anal. Bound. Elem., **36**:3 (2012), 477-491. Zbl 1245.74098
[15] Z. Li, R. Mathon, P. Sermer, *Boundary methods for solving elliptic problem with singularities and interfaces*, SIAM J. Numer. Anal., **24** (1987), 487–498. Zbl 0631.65103
[16] Z.-C. Li, T.-T. Lu, H.-Y. Hu, A.H.-D. Cheng, *Trefftz and collocation methods*, WIT Press, Southampton, 2008. Zbl 1140.65005
[17] Z.-C. Li, H.T. Huang, Y. Wei, A.H.-D. Cheng, *Effective condition number for numerical partial differential equations*, Science Press, Beijing; Alpha Science International Ltd, Oxford, 2014. MR3495915
[18] Z.-C. Li, L.-P. Zhang, Y. Wei, M.-G. Lee, J.Y. Chiang, *Boundary methods for Dirichlet problems of Laplace's equation in elliptic domains with elliptic holes*, Eng. Anal. Bound. Elem., **61** (2015), 91–103. Zbl 1403.65208
[19] D. Palaniappan, *Electrostatoics of two intersecting conducting cylinders*, Math. Comput Modelling, **36**:7-8 (2002), 821–830. Zbl 1036.78006
[20] A. Portela, M.H. Aliabadi, D.P. Rooke, *The dual boundary element method: Effective implementation for crack problems*, Int. J. Numer. Methods Eng., **33**:6 (1992), 1269–1287. Zbl 0825.73908
[21] L.-P. Zhang, Z.-C. Li, M.-G. Lee, *Boundary methods for mixed boundary problems of Laplace's equation in elliptic domains with elliptic holes*, Eng. Anal. Bound. Elem., **63** (2016), 92–104. Zbl 1403.74289

Ming-Gong Lee
Department of Tourism and Leisure/Ph.D. Program
in Department of Civil Engineering,
Chung Hua University,
Hsin-Chu, 30012, Taiwan
Email address: mglee@chu.edu.tw

Li-Ping Zhang
Department of Applied Mathematics,
Zhejiang University of Technology,
Hangzhou, 310023, China
Email address: Corresponding author, zhanglp@zjut.edu.cn

Zi-Cai Li
Department of Applied Mathematics,
National Sun Yat-sen University,
Kaohsiung, 80424, Taiwan
Email address: `zicili1@gmail.com`

Alexander L. Kazakov
Matrosov Institute for System Dynamics and Control Theory
of Siberian Branch of Russian Academy of Sciences,
134, Lermontov str.,
Irkutsk, 664033, Russia
Email address: `kazakov@icc.ru`